

## ARTICLE

**Hydrogel facilitated bioelectronic integration**Richard Vo,<sup>†</sup> Huan-Hsuan Hsu,<sup>†,\*</sup> and Xiaocheng Jiang<sup>\*</sup>Received 00th January 20xx,  
Accepted 00th January 20xx

DOI: 10.1039/x0xx00000x

The recent advances in bio-integrable electronics are creating new opportunities for interrogating and directing biologically significant processes, yet their performance to date is still limited by the inherent physiochemical and signaling mismatches at the heterogenous interfaces. Hydrogel represents a unique category of materials to bridge the gap between biological and electronic systems because of their structural/functional similarity to biological tissues and design versatility to accommodate the cross-system communication. In this review, we discuss the latest progress in the engineering of hydrogel interfaces for bioelectronics development that promote (1) structural compatibility, where the mechanical and chemical properties of hydrogels can be modulated to achieve coherent, chronically stable biotic-abiotic junctions; and (2) interfacial signal transduction, where the charge and mass transport within the hydrogel mediators can be rationally programmed to condition/amplify the bioderived signals and enhance the electrical/electrochemical coupling. We will further discuss the application of functional hydrogels in complex physiological environments for bioelectronic integration across different scales/biological levels. These ongoing research efforts have the potential to blur the distinction between living systems and artificial electronics, and ultimately decode and regulate biological functioning for both fundamental inquiries and biomedical applications.

**1. Introduction**

The relentless evolution of modern electronics is enabling unprecedented capability for information processing and storage. When integrated with biosystems, it allows quantitative interpretation of complex bio-derived signals and dynamic modulation of critical biological functions, empowering influential innovations in glucose monitoring, electrocardiogram and electroencephalogram, cardiac pacemakers, neurostimulators and more.<sup>1-5</sup> Central to the bioelectronic development is the effective and reliable signal transduction across the biotic/abiotic interface – a fundamental requisite that continues to challenge current bioelectronic design and operation, as a result of the intrinsic structural and signaling mismatch between the two distinct systems.

Structurally, traditional electronics are composed of solid-state materials (e.g. metals and semiconductors) that are chemically inert and orders of magnitude stiffer as compared with the soft, bioactive components.<sup>6</sup> This mismatch can adversely affect cell behavior and development, and also lead to insufficient electrode interaction thus large contact impedance and poor signal coupling.<sup>7,8</sup> Particularly, for in-vivo applications, these stiff materials can cause vascular and tissue damage during implantation, and induce foreign body responses and fibrous encapsulation, thus further impeding the quality of cross-system communication.<sup>9,10</sup> Recent progress in

26 nano- and flexible electronics has shown promising  
27 improvement for bio-integration through the reduction of  
28 device dimension<sup>11</sup> and/or substrate stiffness,<sup>12</sup> enabling less-  
29 invasive probe design with intimate and chronically stable bio-  
30 contact for implantable/wearable applications.<sup>13</sup> These  
31 research efforts will continue to benefit from localized  
32 biomaterial engineering at the active recording/stimulation  
33 interfaces to achieve ultimate structural coherence across the  
34 boundary.

35 Functionally, biological and electrical circuits are processing  
36 signals in completely different modality. Biosystems are capable  
37 of transmitting highly complex and dynamic physiochemical  
38 signals *via* water-compliant carriers (such as ions and  
39 biomolecules), while conventional electronics represent  
40 deterministic systems that rely on the controlled transport of  
41 delocalized electrons/holes. The cross-system signaling, which  
42 can be achieved either passively (e.g. with conductive  
43 electrodes) or actively (e.g. with field-effect transistors, or  
44 FETs), remains a limiting factor in device functioning, especially  
45 under physiologically relevant conditions. For example,  
46 electrophysiological recording by microelectrode arrays (MEAs)  
47 can only detect attenuated, spatially-averaged and temporally-  
48 filtered field-potential as a result of poor electrical coupling at  
49 the device interface.<sup>14</sup> Similarly, FET biosensors, which convert  
50 biologically induced potential variation into conductance  
51 changes, typically suffer from compromised signal transduction  
52 in physiological fluids, as a result of charge screening (Debye  
53 length < 1nm in high-ionic strength solutions),<sup>15</sup> signal decay  
54 (due to diffusion/neutralization), and nonspecific binding (by  
55 overwhelming background molecules).

56 Overall, the intrinsic mismatch at the bio-/electronic  
57 interface, both structurally and functionally, is continuously

Department of Biomedical Engineering, Tufts University, Medford, MA 02155, USA.  
E-mail: [Xiaocheng.Jiang@tufts.edu](mailto:Xiaocheng.Jiang@tufts.edu)E-mail: [Huan-Hsuan.Hsu@tufts.edu](mailto:Huan-Hsuan.Hsu@tufts.edu)

† R.V. and H. H. contributed equally to this work.

1 challenging the efficiency and stability of existing devices.<sup>20</sup> 22  
 2 accommodate the mismatch, hydrogel, a three-dimensional<sup>21</sup>  
 3 polymeric network with great structural similarity to biological<sup>24</sup>  
 4 tissues, has been extensively studied as a bridging material<sup>25</sup>  
 5 (Figure. 1). In this review we will discuss the unique properties<sup>26</sup>  
 6 of hydrogel material that can be rationally designed and<sup>27</sup>  
 7 programmed to enhance the structural integration and<sup>28</sup>  
 8 interfacial signaling between biological and electronic system<sup>29</sup>  
 9 and highlight the latest progress in hydrogel-mediated<sup>30</sup>  
 10 bioelectronic development at molecular, cellular, tissue, and<sup>31</sup>  
 11 body levels.<sup>32</sup>

## 12 2. Hydrogel enhanced structural integration

13 Hydrogels are hydrophilic polymer networks that contain up to<sup>35</sup>  
 14 thousands of times their dry weight in water.<sup>16</sup> They have been<sup>36</sup>  
 15 widely recognized for the unique physiochemical properties in<sup>37</sup>  
 16 favor of bio-integration. Mechanically, the stiffness/Young's<sup>38</sup>  
 17 modulus of hydrogels is usually in the range of 0.1-100 kPa.<sup>39</sup>  
 18 Tough hydrogels with stiffness up to MPa have also been<sup>40</sup>  
 19 generated by regulating the composition and crosslinking<sup>41</sup>  
 20 mechanism.<sup>18,19</sup> This range accommodates well with various<sup>42</sup>  
 21 types of cells and tissues<sup>20</sup> to bridge the gap with stiff<sup>43</sup>  
 22 materials.<sup>44</sup>

23 electronics (Figure 1). Chemically, intrinsic or modified surface  
 24 functional groups on hydrogels can provide strong adhesion to  
 25 biological components through non-covalent (e.g. hydrogen  
 26 bonds,  $\pi$ - $\pi$  stacking, and cation- $\pi$  interaction) or covalent  
 27 interactions.<sup>21</sup> Leveraging strategies from emerging biomedical  
 28 research, additional hydrogel features such as porosity/pore  
 29 size,<sup>16</sup> stretchability,<sup>22</sup> water content, topology,<sup>23</sup> and  
 30 conductivity<sup>24</sup> can also be tailored to further control the  
 31 interfacial properties. In general, two types of materials have  
 32 been exploited to form hydrogel: (1) naturally derived polymers  
 33 and (2) synthetic macromolecules. Due to their improved  
 34 uniformity, stability and simplified synthesis/purification,  
 35 synthetic hydrogels provide rational control over physical and  
 36 chemical properties, enabling extensive flexibility in designing  
 37 bioelectronic interfaces based on specific demands.<sup>25,26</sup> For the  
 38 structural integration of bioelectronics, hydrogel has been  
 39 exploited as the interfacing material between biological and  
 40 electronic components<sup>27-28</sup> to improve the structural  
 41 compatibility. For example, hydrogel coatings have been  
 42 extensively applied in epidermal bioelectronics to ensure  
 43 conformal and stable device-epidermis contacts. This hydrogel-  
 44 mediated intimate interface also leads to enhancement in both  
 45 stimulation and recording performances due to reduced gap

# Bio/Electronic Interfaces

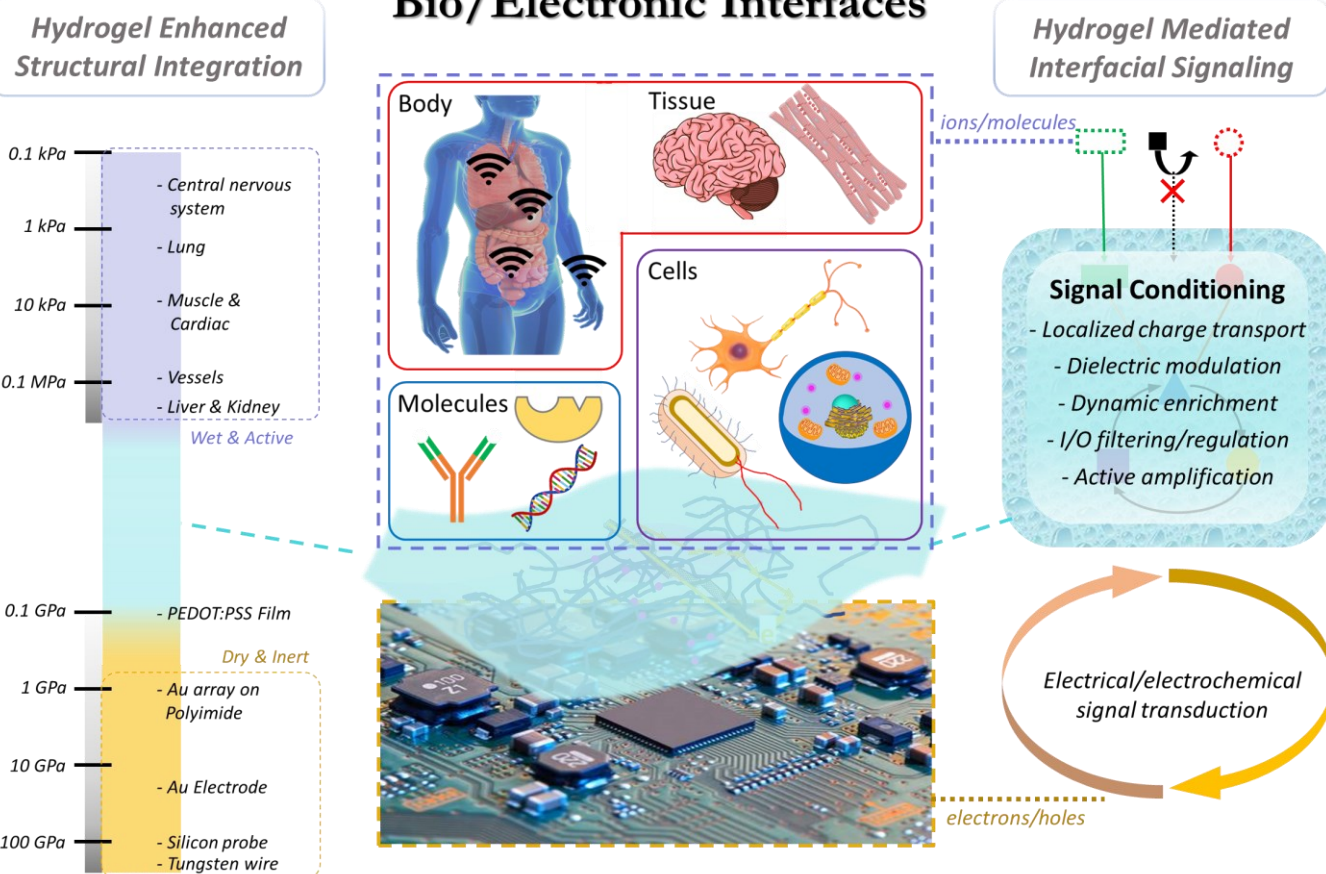


**Figure 1** Hydrogel Facilitated Bioelectronic Integration. **(left)** Structural integration: hydrogel holds unique mechanical and chemical properties to bridge soft, wet, and chemically active biological components with rigid, dry, and inert electronics. Young's moduli of: different biological components (e.g. central nervous system: 0.1-10 kPa; lung: 1-5 kPa; muscle & cardiac: 10-20 kPa; vessels: 125 kPa; liver & kidney: 190kPa), common hydrogels (hydrogel: 0.1-100 kPa; composite hydrogels: 1-100's of kPa; tough hydrogel: ~ MPa) and electronic materials/devices. **(right)** Functional integration: rationally designed hydrogel interfaces enhance the cross-system signal coupling through: (i) facilitating the electron and/or ionic transport; (ii) modulation of local dielectric environment and Debye screening; (iii) dynamic enrichment of molecular biosignals via mass transport control; (iv) regulation/filtering of biological inputs/outputs via programmable hydrogel properties (e.g. pore size/surface charge/chemical affinity); and (v) active signal transduction/amplification via stimuli-responsive hydrogel design.

junction, which will be extensively discussed in the next section.<sup>56</sup> Similarly, hydrogel has found extensive applications in many other bioelectronic designs, such as electroencephalogram,<sup>57</sup> electrocardiogram, transcutaneous electrical nerve stimulation,<sup>58</sup> electronic skin, and highly stretchable wearable devices.<sup>29,30,31</sup>

Different from skin, the integration of bioelectronic devices with internal biological systems typically requires invasive procedures, where immune responses and scar formation around electronics are a common barrier to electrical recording and stimulation. Soft cells/tissues have a Young's modulus in the range of 0.5 to 100's of kPa,<sup>32,33</sup> whereas typical electronic materials (e.g. gold, silicon, etc.) are closer to 100's of GPa.<sup>34</sup> These differences cause considerable damage to surrounding tissue after electronic implantation due to local mechanical strain.<sup>35</sup> Furthermore, immediately after contact, proteins adsorb to the electronic surface due to their hydrophobicity and lack of bioactive functional groups. The protein adsorption then activates immune signaling cascades and pro-inflammatory responses, inducing complex cellular responses to the device.<sup>36</sup> This foreign body response can increase the impedance at the tissue/electrode interface that challenges the electrical signal transduction.<sup>36,37,38</sup> Therefore, harmonizing the mechanical mismatch between tissue and electronics is important for improving device performance. Recently, hydrogel coatings have been utilized to improve the long-term biocompatibility of stiff electronic devices by reducing the large mechanical mismatch to minimize the immune response.<sup>39,40</sup> Furthermore, the physical properties of the hydrogel may be tuned to match the local biological environment in order to elicit normal behavior after integration with electronics. As the mechanical forces acting on cells and tissues can greatly affect their function and behavior,<sup>41,42</sup> by modifying composition and crosslinking density, hydrogels have been engineered to have tissue-like mechanical properties for improving bioelectronic integration. For example, polyethylene glycol dimethacrylate hydrogel with stiffnesses similar to brain tissue (1.6 kPa to 171.5 kPa) has been coated on implanted electrodes of brain tissues.<sup>43</sup> These hydrogel coatings significantly reduced the local strain caused by the large mechanical mismatch between brain tissue and metal electrodes, and micromotion of brain tissue relative to the stationary implanted device. The decrease in strain resulted in a reduction of the glial scar formation surrounding the implantation site compared to uncoated devices.<sup>44</sup>

Overall, hydrogels provide a wide selection in compositions, structures, and functions, which offers unique advantages in the customization of bioelectronic interfaces for modifying electronics to accommodate various biological components,<sup>45</sup> hence, advancing the quality and satiability of existing tools for the physiological signal recording/simulation of human tissues.<sup>46</sup> Recent development in the hydrogel-coated bioelectronics for *in-vivo* applications were systematically reviewed by Yuk et al.<sup>47</sup>

muscles), which is mediated by ion fluxes and cell membrane potential changes; and (2) biochemical signaling, where (bio)molecules transmit and trigger internal reaction cascades (e.g. metabolism, immune response, tissue regeneration). Coupling these two distinct signaling pathways at bioelectronic interface will allow comprehensive modulation/interrogation of biofunctions through electrical inputs/outputs. However, challenges remain in establishing an effective yet reliable cross-system signal coupling at bio-electronic interfaces, which can be summarized into following three aspects: (1) the physiochemical mismatch between both systems can prohibit the intimate contacts and lead to signal attenuation (ion/molecule diffusions); (2) The physiological fluid presents a high-ionic strength environment with large amount of background molecules that jeopardizes the efficiency and accuracy in signal transduction; (3) Bio-recognition components (such as enzymes, antibodies, bio-receptors) that have been used to facilitate biochemical signal transduction usually hold limited lifespans owing to the bio-incompatible immobilization techniques. Toward overcoming these challenges, hydrogel represents a unique interfacing material as it provides a biologically relevant microenvironment with tunable mass and/or charge transport properties. The state-of-the-art achievements of the implementations of hydrogels in improving the bioelectronic signal coupling are reviewed in following sections.

### 3.1 Bioelectrical signaling

In electrically active cells and tissues (e.g. neurons, muscle cells, cardiomyocytes etc.), the selective ion transport across cell membrane and correspondent membrane potential changes are central to the generation and transmission of bioelectrical signals. The continuous recoding and comprehensive interpretation of these signals can greatly elevate our understanding in important biological processes;<sup>44,45</sup> while stimulation of these tissues finds critical importance for both physiological studies and disease treatments.<sup>46</sup> Hence, many state-of-the-art developments in bioelectronics are targeting at improving the bi-directional communication between these tissues and external electronics. Generally, the electrical recording/simulation of excitable tissues are completed by the conversion between ion- and electron-mediated electrical signals. At the tissue-electronic interface, equilibrant electrolyte-electrode interactions (ion diffusion, redox reaction, electrical double layer, etc.) can establish a semi-stable electrical potential. During recording, the ion flux varies the electrical potential and consequently induces the electron flow in electronics to be detected. In contrast, during stimulation, applying an external electric field can trigger ion re-distribution at the tissue-electronic interface, altering the membrane potential of excitable cells, and activating ion channels.

## 3. Hydrogel mediated bio-signal transduction

The functions of living systems relies on highly sensitive, dynamic, and error-tolerant transduction of complex bio-signals through: (1) bioelectrical signaling (e.g. in brain, heart, and

As both bioelectrical recording and stimulation are associated with the highly localized, transient ion flux, intimate and chronically stable tissue-electronic contact becomes critically important to effective interfacial signaling. However, as discussed earlier, the intrinsic mismatch of mechanical and chemical properties limits the quality of tissue electronic contacts. Hydrogels have been used as coatings encapsulating materials on the electrode surface to bridge the structural mismatch between electronics and electrically active tissues.<sup>17</sup> While demonstrating improved biocompatibility, the insulating nature of hydrogel impedes the signal transduction between bio- and electronic- systems. Although hydrogels hold certain degrees of ionic conductivity<sup>47</sup> that can be further enhanced by introducing high concentration ionic solutions such as ionic liquids and buffers into hydrogel matrix,<sup>48,49</sup> the stability of such ionic conductivity can be disturbed by continuous ion diffusion. Consequently, the performance of hydrogel-coated devices is limited, especially for chronic applications. To overcome this limitation, conductive hydrogels that display both tissue-like mechanical properties and electrical conductivity have been developed by incorporating different conductive fillers such as graphene, carbon nanotubes, gold/silver nanoparticles, or conductive polymers into the hydrogel network.<sup>50-54</sup> In particular, PEDOT:PSS has been widely used in fabricating conductive hydrogels for bioelectronic applications due to its high electrical conductivity and solution-based processing capabilities.<sup>22,55,56</sup> Liu et al. reported soft micropillar electrodes composed of electrically conductive hydrogel with tissue-like stiffness for electrophysiological recording of HL-1 cardiomyocytes.<sup>55</sup> The soft conductive hydrogel electrodes were composed of PEDOT:PSS modified with ionic liquid and exhibited a Young's modulus of 13.4 kPa. The soft nature of the electrodes allowed for accommodation of the movements of cardiomyocytes during beating (Fig. 2a). Furthermore, this conductive hydrogel reduced the impedance at the tissue-electronic interface and improve transduction of electrophysiological signals (Fig. 2b).

Altogether, this hydrogel electrode demonstrated a greater quality in recorded signals in terms of both amplitude and larger signal-to-noise ratio compared to metal electrodes with stiffness of 100 GPa (Fig. 2c). Moreover, Yuk et al. developed a method for 3D printing PEDOT:PSS polymers that can be used to form conductive hydrogels.<sup>57</sup> After printing and annealing, the dry 3D-printed polymer exhibits conductivity over 155 S cm<sup>-1</sup>. The conductive polymer can be converted into hydrogel by swelling in aqueous solution. In the hydrogel state, the Young's modulus was reported at 1.1 MPa and electrical conductivity of 28 S cm<sup>-1</sup>. This approach was utilized to fabricate soft probes for *in vivo* recording of neurons over a 2-week period (Fig. 3a-c). Dalrymple et al. demonstrated the advantages of conductive hydrogel coated platinum electrodes versus bare platinum electrodes implanted in rat cochlea.<sup>54</sup> PEDOT was incorporated into a PVA hydrogel as a conductive hydrogel coating and electrodes were implanted over a 5-week period. The coated electrodes showed significant improvement of electrical properties, displaying significantly higher charge storage capacity, charge injection limit and lower impedance. The effective long-term integration of bioelectronic devices *in vivo* is vital for communication with the body. These works present the use of hydrogel to facilitate structural integration and improve signal coupling at the bioelectronic interface. Thus, engineering of both hydrogel and device properties to match the biological environment offers the potential to overcome the challenges of immune response caused device failure.

In addition to common conductive hydrogels, composite hydrogels have been developed to provide additional versatility in bio-integration due to its tunable soft, conductive, and elastic properties. For example, an interpenetrating hydrogel network composed of both poly(3,4-ethylenedioxothiophene) polystyrene sulfonate (PEDOT:PSS) and polyacrylic acid hydrogels was electrically conductive and highly elastic, capable of stretching over 100% strain while maintaining conductivity.<sup>56</sup> The stiffness could be tuned between 8 and 374 kPa by changing the polymer concentrations, making it applicable to match a

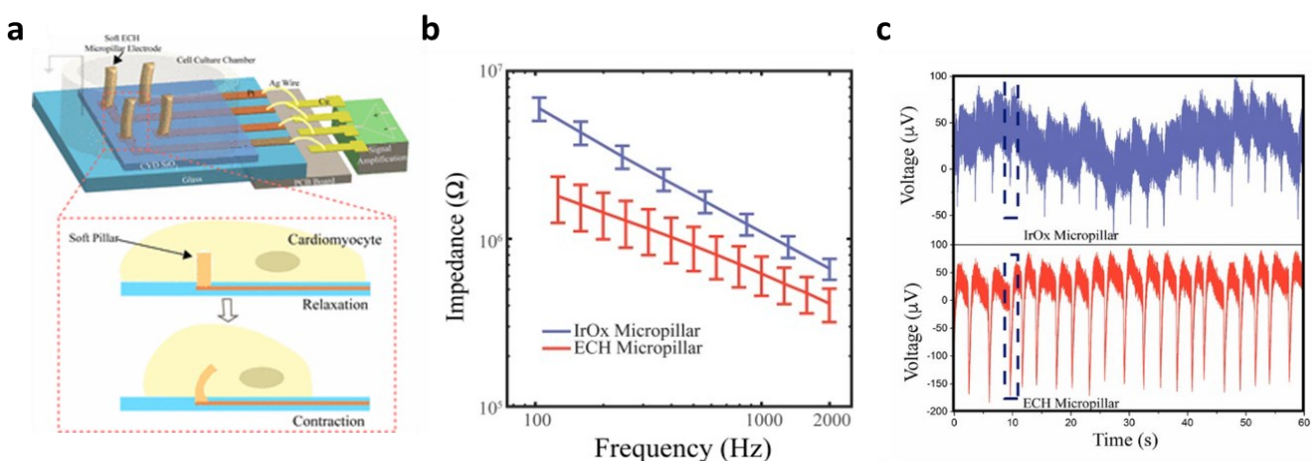


**Figure 2.** Comparison between soft hydrogel probes and rigid metal electrodes for interfacing with beating HL-1 cardiomyocytes. (a) Schematic of soft conductive micropillars for electrophysiological recording of HL-1 cardiomyocytes during spontaneous beating. (b) Impedance measurements of metal micropillar (blue) compared to conductive hydrogel micropillars (red). (c) Extracellular recording of cardiomyocyte activity from conventional metal electrode (top) and soft conductive hydrogel micropillar (bottom). Reproduced with permission from ref. 55. Copyright (2018) National Academy of Sciences.

1 wide range of biological tissue. Similarly, Liu et al. demonstrated  
 2 a 64 channel array of hydrogel electrodes for interfacing with  
 3 beating hearts for electrophysiological recording *in vivo* (Fig. 3d).<sup>58</sup> The electrodes of this array are designed to be  $<100\text{ }\mu\text{m}$   
 4 for potential single cardiomyocyte recording and possess tissue-  
 5 like Young's modulus and elasticity, which enable a stable  
 6 interface with beating cardiac tissue *in vivo* (Fig. 3e).  
 7 Additionally, the device was glued to the heart using a  
 8 bioadhesive for strengthening hydrogel-heart integrations. This  
 9 strategy can provide stable signal recording during heart  
 10 beating and leads to the improvement in signal quality (Fig. 3f).  
 11 Moving forward, composite hydrogels may be further  
 12 engineered for additional functions, such as eluting bioactive  
 13 substances (i.e. growth factors or drugs). For example, a  
 14 multifunctional hydrogel coating incorporated with both  
 15 conducting polymers and anti-inflammatory drugs was used for  
 16 improving the interface of neural cuff electrodes.<sup>59</sup> The device  
 17 displayed significantly increased axon density and decreased  
 18 scar tissue formation in the surround area compared to control  
 19 groups, and was capable of recording and stimulating over 5  
 20 weeks. These works demonstrate the potential of hydrogel  
 21 bioelectronics for long-term *in vivo* use by matching the  
 22 mechanical properties of the device to the *in vivo* environment  
 23 and attenuating the immune response. Overall, the extensive  
 24 tunability offered by electrically conductive hydrogels have  
 25 great potential for use in implantable bioelectronics. By utilizing  
 26 the tissue-like properties of hydrogel with the electrical  
 27 properties of conducting polymers, conductive hydrogels  
 28 enable improved structural integration and signal coupling.  
 29

### 3.2 Biochemical signaling

32 Many biological functions including sensation, metabolism,  
 33 immune response, etc., are mediated by a series  
 34 biomolecular interactions such as enzymes, membrane/nucleic  
 35 receptors, and antibodies/immunoglobulin receptors. The  
 36 precise interpretation of these complex biochemical signals in  
 37 the quantitative electrical language will provide unique insight  
 38 about the underlying biological function. Electrochemical  
 39 methods have been widely used for bio-to-electronic signal  
 40 transduction. In particular, with the incorporation of biorecognition  
 41 molecules that either (1) selectively convert the  
 42 target analyte into electroactive species or (2) selectively bind  
 43 to the target analyte, the electrochemical sensors can  
 44 specifically translate corresponding biological events in the  
 45 form of current, potential or impedance changes.  
 46 A comprehensive review in electrochemical bioelectronics is  
 47 presented by Ronkainen et al.<sup>60</sup> Alternatively, FETs possess  
 48 unique capability to actively sense and amplify the variation of  
 49 electrical potential at the device surface. When integrated with  
 50 bio-recognition molecules such as enzymes, antibodies, and  
 51 single-strand DNA, the selective binding of the target molecule  
 52 or the generation of biologically derived species induces  
 53 change in local charge and the biological event is transduced  
 54 into an electrical signal in real time. This capacity makes FETs  
 55 excellent candidate for coupling electronic- and living- signals.  
 56 While both types of detection mechanisms have been widely

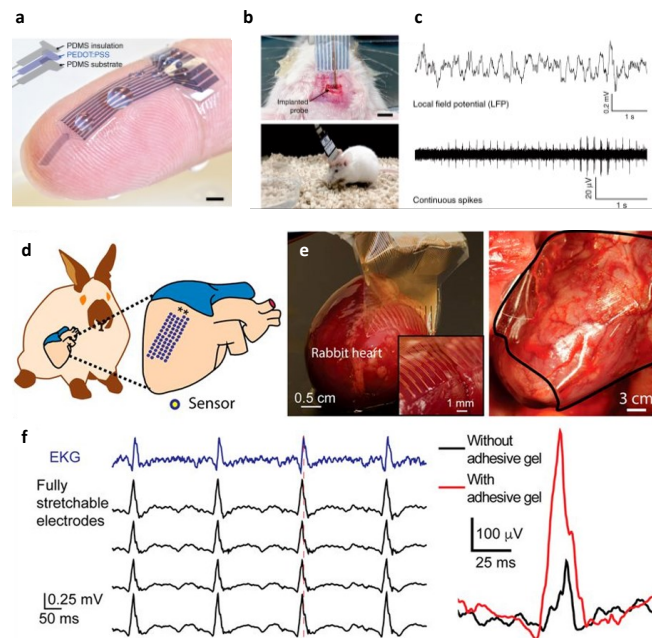


**Figure 3.** Hydrogels for *in vivo* tissue-electronics interfacing. (a) Image of 3D printed soft neural probe. Scale bar, 2 mm. (b) Images of probes implanted in mouse. (c) Continuous measurement of local field potential (top) and extracellular action potentials (bottom). Reproduced with permission from ref. 57. Copyright (2020) Springer Nature. (d) Schematic of stretchable hydrogel electrode array placed on heart. (e) Images of hydrogel electrode array conforming to a rabbit heart. Right: Voltage trace from hydrogel electrodes with (red) and without (black) bioadhesive gel. Reproduced with permission from ref. 58. Copyright (2020) National Academy of Sciences.

investigated, challenges remain to further improve the signal transduction at bio-electronic interfaces, especially under physiologically relevant conditions:

First, interfacial signal attenuation becomes significant as the bioderived molecules are quickly diluted and/or neutralized before meaningful information can be transmitted to the electronics, demanding extremely intimate bio-electronic interfaces.<sup>61,62,63</sup> In particular, for FET sensing, signal attenuation is aggravated by the presence of a high-concentration of electrolytes, which induce electrostatic screening.<sup>64</sup> The strength of the electrical field generated by charged analytes is diminished at a distance of 0.75 nm in physiological environments. Although diluted buffer solutions, desalting, or purification can increase the Debye screening length, post-processing compromises the real time sensing capabilities of bioelectronics.<sup>65</sup> Shorter bioreceptors such as truncated antibodies<sup>66</sup> and aptamers<sup>67,68</sup> have also been exploited to overcome the charge screening effect, but their application is typically limited by their complex design/synthesis.

Second, nonspecific binding of background species such as serum albumin can induce significant false signals or biofouling to interfere with the functioning of bioelectronics. Effective filtering of competing biochemical signals has the potential to improve the device performance in both sensitivity & selectivity. Existing strategies (e.g. pre-absorption of blocker proteins<sup>69</sup> or hydrophilic/hydrophobic modifications) could reduce the non-specific binding of certain biomolecules, but

1 lack the capability to regulate the accessibility of dynamic biochemical signals in general.<sup>70</sup> 58  
2 59

3 Lastly, the chronic performance of bioelectronics is 58  
4 compromised by the limited lifetime of bio-recognition 59  
5 components, which lose their activity quickly as a result of fast 6  
6 and progressive chemical/structural degradation in non-native 7  
7 environment. This issue is further amplified by the bio- 8  
8 incompatible functionalization strategies such as physical 9  
9 adsorption or chemical conjugation.<sup>61</sup> Physical adsorption 10  
10 usually relies on van der Waals or electrostatic interactions.<sup>62</sup> 11  
11 However, these weak interactions can lead to desorption of 12  
12 biomolecules and loss of sensitivity over time.<sup>63</sup> Chemical 13  
13 conjugation generates a strong and stable biomolecule 14  
14 attachment through covalent bonding,<sup>71</sup> but typically 15  
15 compromise the bioactivity due to the disturbance of the native 16  
16 structure.<sup>72</sup>

17 Toward overcoming these mismatches, hydrogels have 18  
18 been utilized to immobilize molecular biomachinery such as 19  
19 enzymes or antibodies for functionalizing electronics.<sup>73</sup> The 20  
20 "hydrogel biotransducer" demonstrates abilities in (1) 21  
21 modifying the local dielectric environment thus increasing 22  
22 Debye screening length;<sup>15,74</sup> (2) regulating the "input" and 23  
23 "output" biosignals through mass transport control,<sup>75</sup> which 24  
24 reducing nonspecific absorption/interactions of interference 25  
25 species<sup>75,76</sup> while enriching/amplifying the bio-transformed 26  
26 signal; and (3) providing a biologically relevant 27  
27 microenvironment for maintaining the functions of immobilized 28  
28 biomachinery, through mild, biocompatible fabrication 29  
29 processes. Recent developments in hydrogel enabled structural 30  
30 integration and signal coupling between biomolecules and 31  
31 electronics are summarized in following sections. 60

32 Enzymatic transformation has been widely explored 61  
33 in electrochemical based sensor design, where hydrogel can 62  
34 preserve the activity of encapsulated enzymes<sup>77</sup> while providing 63  
35 sufficient porosity to facilitate the contact between electrodes<sup>64</sup> 64  
36 and enzymatic products. Furthermore, the 3-D matrix<sup>65</sup> 65  
37 hydrogel can also increase the encapsulation efficiency<sup>66</sup> 66  
38 enzymes compared to planar electrodes, increasing the<sup>67</sup> 67  
39 amplitude of generated biosignals. These features make<sup>68</sup> 68  
40 hydrogel an excellent candidate for enzyme-electronic<sup>69</sup> 69  
41 integration. For example, by immobilizing lactate oxidase inside<sup>70</sup> 70  
42 dimethylferrocene-modified poly(ethylenimine) hydrogel while<sup>71</sup> 71  
43 incorporating bilirubin oxidase-based cathode, Hickey et<sup>72</sup> 72  
44 fabricated a self-powered lactate biosensor with a detection<sup>73</sup> 73  
45 range between 0 - 5 mM with a sensitivity of 45<sup>74</sup> 74  
46  $\mu\text{A}/\text{mM}\cdot\text{cm}^2$ .<sup>78</sup> Additionally, Wang et al. immobilized alcohol<sup>75</sup> 75  
47 oxidase and glucose oxidase onto the electrodes using chitosan<sup>76</sup> 76  
48 hydrogel. These hydrogel-based biosensors present the ability<sup>77</sup> 77  
49 to detect alcohol and glucose in bodily fluids by measuring<sup>78</sup> 78  
50 electric currents produced by the enzymatic reactions.<sup>79,80</sup> 79

51 To enable multiplexed sensing capability, Yan et<sup>80</sup> 80  
52 fabricated a biosensor array through a multistep<sup>81</sup> 81  
53 photopolymerization to immobilize glucose oxidase and lactate<sup>82</sup> 82  
54 oxidase on separated microelectrodes. This device<sup>83</sup> 83  
55 demonstrates simultaneous detection of glucose and lactate<sup>84</sup> 84  
56 with sensitivity of  $0.9 \mu\text{A}\cdot\text{cm}^{-2}\cdot\text{mM}^{-1}$  and  $1.1 \mu\text{A}\cdot\text{cm}^{-2}\cdot\text{mM}^{-1}$ ,<sup>85</sup> 85  
57 respectively.<sup>27</sup> Li et al. also demonstrated the multiplex<sup>86</sup> 86

detection of different biomarkers by functionalizing electrodes with hydrogels through multi-step inkjet printing.<sup>81</sup> By loading

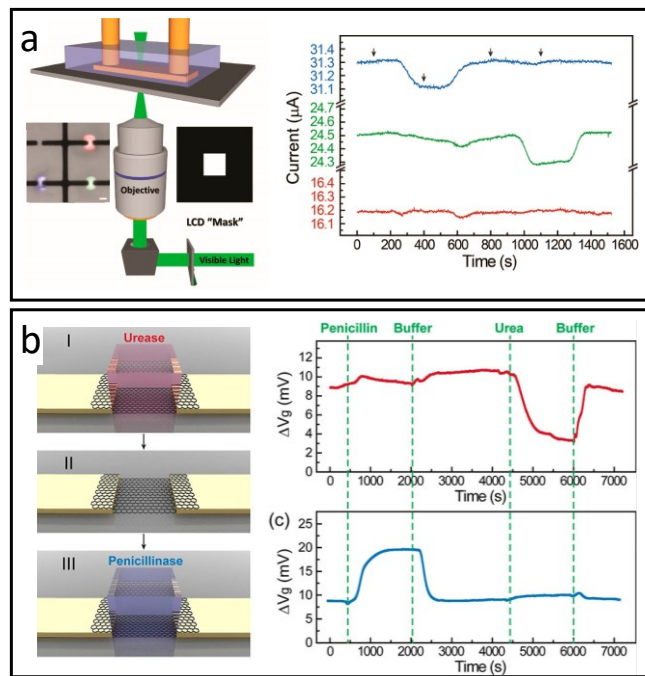


**Figure 4.** Designs of multifunctional- hydrogel-based- bioelectronics: (a) left: Schematic of projection lithography setup for hydrogel patterning. (a insert) Image of hydrogels containing red, blue, and green fluorescence dyes. Scale bar, 20  $\mu\text{m}$ . Right: Multiplex sensing of penicillin (blue), acetylcholine (green) and no-enzyme control (red). Reproduced with permission from ref. 76. Copyright (2019) American Chemical Society. (b) Left: schematic of hydrogel-enabled modularized FET. Right: performance of modularized FET biosensor functionalized by urease-encoded hydrogel (red) and penicillinase-encoded hydrogel (blue). Reproduced with permission from ref. 75. Copyright (2019) American Chemical Society.

the printer cartridges with different bio-inks, electrodes were independently functionalized with different enzymes sensitive to glucose, lactate, and triglycerides. The sensors perform similarly in both phosphate buffer and serum solutions, which indicates that hydrogel can minimize the interference from background metabolites and molecules. Besides, the fabrication using ink-jet printing represents the possibility for mass production of biosensors with customized biomarker functionalization.

Similarly, Bay et al. created a multi-functional FET array using projection microlithography with diffraction-limited spatial resolution. In this design, enzyme functionalized polyethylene diacrylate (PEGDA) hydrogels were individually crosslinked on top of graphene FET by controlling the area of light exposure with inverted microscope and computer-controlled photomask (Fig. 4a). Multiplex detection was demonstrated by sequential photopolymerization of hydrogels containing enzymes for the specific detection of penicillin or acetylcholine (Fig. 4a). The hydrogel encapsulation was also shown to extend the activity of penicillinase up to 7 days compared to only several hours in solution. Additionally, the

1 PEGDA hydrogel was found to significantly reduce the  
 2 nonspecific absorption of bovine serum albumin (BSA, MW 6.65  
 3  $\times 10^4$  g/mol) to the FET surface.<sup>76</sup> To further improve the design  
 4 flexibility, Dai et al. demonstrated the modular version of  
 5 hydrogel-gate FETs made of independently fabricated enzyme  
 6 functionalized hydrogels and electronic transducer that can be  
 7 reversibly assembled/disassembled.<sup>75</sup> In this work, hydrogels  
 8 containing urease and penicillinase were fabricated in a mold  
 9 and then integrated onto FET. The enzymatic reaction is highly  
 10 confined within the hydrogel environment, accumulating within  
 11 and slowing the diffusion to the external buffer environment.  
 12 This local signal amplification allows for sensing without the  
 13 permanent surface modification of the FET device and enables  
 14 the ability to reprogram or replenish the bioreceptors by  
 15 switching hydrogels without affecting the device sensitivity (Fig.  
 16 4b).

17 For active transducers like FET, another critical challenge is  
 18 associated with electrostatic screening as the signal  
 19 transduction is achieved through biologically induced changes  
 20 in local electrical field. This becomes particularly challenging in  
 21 physiological environment, where effective detection range (or  
 22 Debye length) is within the nanometer length-scale.<sup>82</sup> By  
 23 modifying the local dielectric environment and modulate the  
 24 charge distribution, hydrogel provides a promising solution to  
 25 reduce electrostatic screening for high-sensitivity FET detection  
 26 in physiological fluids without pre-processing. For example,  
 27 Lieber and colleagues presented that the Debye screening  
 28 length of both silicon nanowire- (SiNW) and graphene- based  
 29 FET can be significantly increased by PEG hydrogel  
 30 functionalization.<sup>15,74</sup> First, SiNW-FET modified by PEG hydrogel  
 31 successfully detected prostate specific antigen (PSA) in  
 32 phosphate buffer solutions (PBS) with concentrations as high as  
 33 150 mM, whereas FETs without PEG could only detect PSA in  
 34 PBS concentrations lower than 10 mM (Fig. 5a). Concentration-  
 35 dependent measurements also demonstrates that in 100 mM  
 36 PBS, PEG modified SiNW-FET is able to hold linear response to  
 37 PSA in the range of 10 to 1000 nM when implemented<sup>58</sup>  
 38 Similarly, PEG-modified graphene FETs also exhibited real-time<sup>59</sup>  
 39 reversible detection of PSA from 1 to 1,000 nM in 100 mM PBS<sup>60</sup>  
 40 In addition, co-modification of graphene FET with PEG and PSA<sup>61</sup>  
 41 aptamers enabled the sensitive yet reversible detection of PSA<sup>62</sup>  
 42 since (1) the conformational changes of these highly charged<sup>63</sup>  
 43 aptamers upon PSA binding led to a significant change in electric<sup>64</sup>  
 44 field of graphene gate and (2) aptamers own reversible binding<sup>65</sup>  
 45 ability with PSA without loss of activity (Fig. 5b).<sup>74</sup> Additional<sup>66</sup>  
 46 recent advancements in bio-stimuli responsive smart hydrogels<sup>67</sup>  
 47 represent an alternative strategy to overcome the by active<sup>68</sup>  
 48 transducing and amplifying the biomolecular binding within the<sup>69</sup>  
 49 hydrogel matrix. For example, hydrogels made of mannose and<sup>70</sup>  
 50 N, N-dimethylacrylamide that undergoes volume change<sup>71</sup>  
 51 response to the formation of lectin-mannose molecule<sup>72</sup>  
 52 complex are applied as gate materials for fabricating FET-based<sup>73</sup>  
 53 lectin sensors. The change in hydrogel volume can introduce<sup>74</sup>  
 54 shift in local electrical field at gate electrode, which can be<sup>75</sup>  
 55 detected by the FET.<sup>83</sup> Many smart hydrogels have been<sup>76</sup>  
 56 developed recently, including antigen-<sup>84</sup> nucleic acid-<sup>85</sup> and<sup>77</sup>  
 57 enzymatic reaction- responsive hydrogels.<sup>86</sup> We believe that<sup>78</sup>

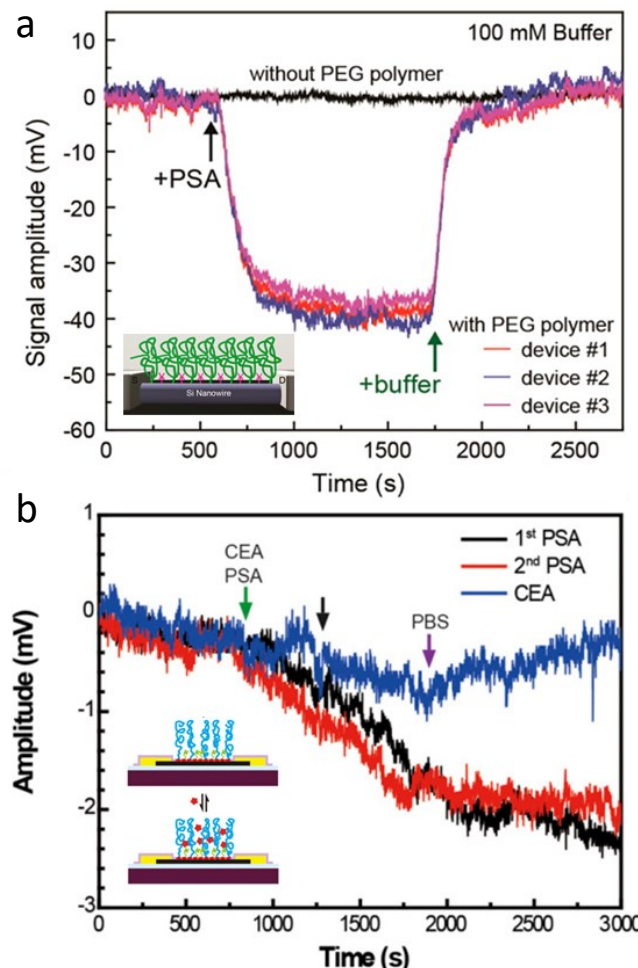


**Figure 5** Hydrogel coating for reduced charge screening. (a) PEG modified SiNW-FET, which demonstrated reversible detections of PSA antigen in 150 mM PBS solution, while FET without PEG showed no signal. Reproduced with permission from ref. 15. Copyright (2015) American Chemical Society. (b) graphene FET co-modified with PEG and PSA aptamers, which exhibited real-time reversible detection of PSA from 1 to 1,000 nM in 100 mM PBS. Reproduced with permission from ref. 74. Copyright (2016) National Academy of Sciences.

functions of molecular-level bioelectronics can be broaden to a new level through further explore possibility in smart hydrogel-electronics integration.

In hydrogel transducers, mass transport inside the hydrogel matrix determines the accessibility of ions and molecules to the FET gate, providing additional control over device sensitivity and selectivity based on specific demands. In general, the mass transport properties of hydrogel material can be regulated by tuning the molecular weight of monomer,<sup>87</sup> cross-linking density,<sup>88</sup> or through the introduction of specific-sized porogens.<sup>89</sup> In the modular FET design presented earlier<sup>94</sup>, for example, the diffusion of methylene blue (MB, MW 320 g/mol) exhibit substantially varied rate in hydrogels crosslinked from PEGDA, gelatin methacrylate (GelMA), and alginate, as a result of the difference in pore size (Fig. 6a insert).<sup>75</sup> Correspondently, FET functionalized with GelMA shows a 4 mV signal after the introduction of poly-L-lysine (PLL) solution, while the same PLL solution cannot induce a detectable signal in PEG functionalized FET (Fig. 6a).<sup>75</sup> This difference in mass transport demonstrates significant effect in preventing the nonspecific binding from large biomolecules with hydrogel-gate design. Similar results

1 have also been demonstrated in the research of Burrs et al.,<sup>36</sup> which, alcohol oxidase was immobilized onto a nanoplatinum<sup>37</sup> 2 graphene-modified electrode using hydrogel made of chitosan<sup>38</sup> 3 poly-N-isopropylacrylamide (PNIPAAm), silk fibroin, and<sup>39</sup> 4 cellulose nanocrystals. The results demonstrated that high<sup>40</sup> 5 porosity of chitosan and PNIPAAm hydrogels can lead to better<sup>41</sup> 6 sensitivity and faster response time during alcohol sensing.<sup>42</sup> 7 Also, Kim et al. demonstrated the PEG hydrogel<sup>43</sup> 8 functionalization of interdigitated microelectrodes for the<sup>44</sup> 9 detection of amyloid beta 42 (A $\beta$ <sub>42</sub>, 2.2 nm diameter) and<sup>45</sup> 10 prostate-specific antigen (PSA, 4.1 nm diameter) via antibody<sup>46</sup> 11 antigen binding.<sup>91</sup> The hydrogel porosity was adjusted between<sup>47</sup> 12 two sizes, "loose" and "dense," by tuning the molecular weight<sup>48</sup> 13 of PEG monomers. The dense hydrogel enabled the diffusion of<sup>49</sup> 14 A $\beta$ <sub>42</sub> selectively, where the diffusion of PSA was inhibited.<sup>50</sup> 15 Detections of PSA was achieved on devices functionalized by<sup>51</sup> 16 loose hydrogel where the diffusion of PSA results in signals<sup>52</sup> 17 twice greater than both dense hydrogel- and non- modified<sup>53</sup> 18 devices (Fig. 6b). Besides, the results indicated that the hydrogel<sup>54</sup> 19 functionalization also increased the device sensitivity, owing to<sup>55</sup> 20 its three orders of magnitude increasing in immobilized<sup>56</sup> 21 antibodies as compared to electrodes without hydrogel.<sup>57</sup> 22

23 In addition to mass transport, the chemical properties<sup>58</sup> 24 hydrogel can be tuned to achieve selective diffusion<sup>59</sup> 25 molecules with a certain charge or chemical affinity.<sup>92</sup> This<sup>60</sup> 26 general strategy could serve to promote the real-time and label<sup>61</sup> 27 free detection of analytes in physiological solutions. The<sup>62</sup> 28 additional selectivity can increase the functionality of the<sup>63</sup> 29 bioelectronics for real-time sensing applications, potentially<sup>64</sup> 30 decreasing the need for pretreating samples to remove<sup>65</sup> 31 background species or significantly reducing biofouling and<sup>66</sup> 32 nonspecific adsorption for in vivo implantation. Besides,<sup>67</sup> 33 computational modeling could provide useful insight about the<sup>68</sup> 34 interfacial transport processes<sup>93,94</sup> which will further assist the<sup>69</sup> 35 hydrogel design for both signal enrichment and reduced<sup>70</sup>

nonspecific binding. Due to these unique advantages in hydrogel functionalization, various bioreceptors have been incorporated with the hydrogel-based bioelectronics to transduce biological signals such as femtomolar levels of disease antibodies, nucleic acids, and single viruses.<sup>95-97</sup> These approaches have opened many new opportunities in bioelectronics for biosensing, implantable stimulators, drug screening, disease models, brain-machine interfaces and more.

## 4. State-of-the-art applications of hydrogel-based bioelectronics

### 4.1 Tissue-electronic interfaces

Hydrogels have been widely utilized as soft, bioactive coatings, or 3-D constructs to improve the integration of cells with synthetic substrates/scaffolds, which can promote cell adhesion, proliferation, and lifetime.<sup>98-100</sup> In the context of bioelectronics, hydrogel mediators have been found to benefit cell functioning and bi-directional signaling for both electroactive- (e.g. neurons<sup>101,102</sup>, cardiomyocytes<sup>103,104</sup> etc.) and non-electroactive- cells (macrophages,<sup>105</sup> HeLa cancer cells,<sup>106</sup> etc.). In terms of electroactive cells, hydrogels offer superior biocompatibility to maintain their morphology and functions such as metabolism, proliferation and differentiation, while providing sufficient porosity to ensure the transduction of physiological signals. For example, a fibrin-based hydrogel was used as a soft substrate for integrating human induced pluripotent stem cell (iPSC) derived cardiomyocytes with nanomesh probes.<sup>103</sup> The soft mechanical and elastic properties of both the hydrogel and probes allowed cardiomyocytes to perform contraction and relaxation motions comparable to the one without nanomesh attachment. This device enabled the recording of electrophysiological signals of the cardiomyocytes over 96 hours without significant cell damage. Moreover, Kujala

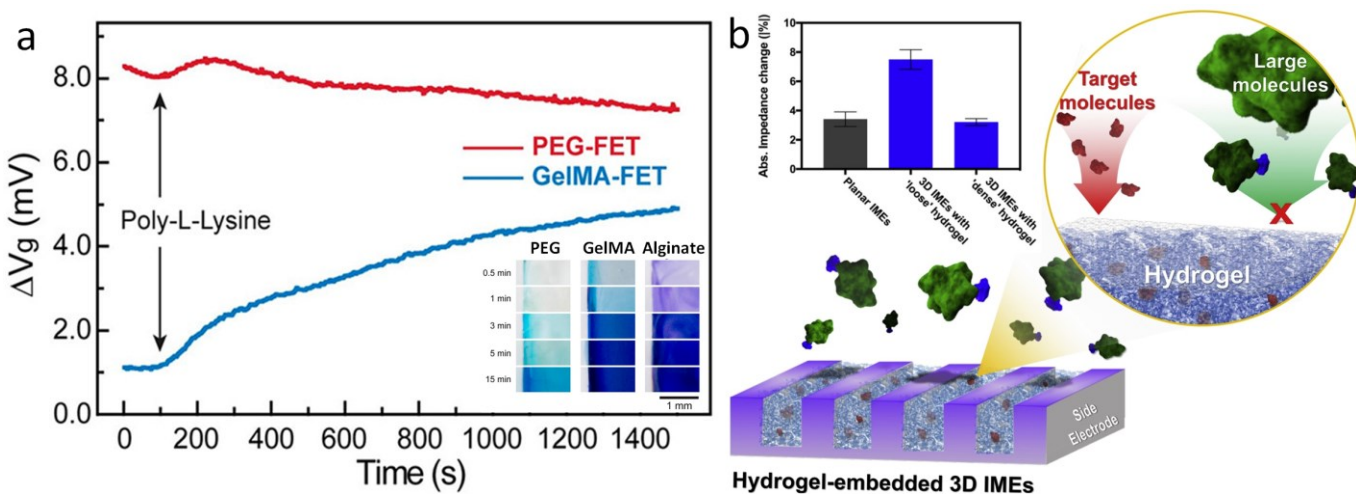


**Figure 6.** Bio-signal filtering by modulating the mass transport of hydrogel matrix. (a) Compositional controls: poly-L-lysine nonspecific binding tests on FET passivated with PEG (red) and GelMA hydrogel. Results indicated that PEG can effectively prevent external noise from poly-lysine due to its small pore size/low mass transport. Insert: Diffusion of methylene blue inside PEG, GelMA, and alginate hydrogel over time. Results present the influence of different hydrogel components in mass transport. Reproduced with permission from ref. 75. Copyright (2019) American Chemical Society. (b) Schematic of electrodes functionalized with hydrogel. Insert: Impedance changes in planar electrodes and with dense and loose hydrogel by binding of A $\beta$ <sub>42</sub>. Insert: Impedance changes in planar electrodes and with dense and loose hydrogel by binding of PSA. Reproduced with permission from ref. 91. Copyright (2020) Elsevier.

1 et al. applied micro-molded gelatin hydrogel to integrate 32  
 2 cardiomyocytes with microelectrode arrays. On this device, the 33  
 3 immobilized cells were able to develop normally to form 34  
 4 laminar cardiac tissues, which were then exploited 35  
 5 to investigate the pharmacological effects of  $\beta$ -adrenergic agonists 36  
 6 and terfenadine in human cardiac cells with 37  
 7 electrophysiological recording.<sup>104</sup> The latest developments 38  
 8 in this direction have been discussed in the review article 39  
 9 published by Kitsara et al. and Fattah et al.<sup>107,108</sup> 40

10 In addition to cell/tissue recording on planar substrates 41  
 11 there have been substantial on-going effort towards 42  
 12 construction of 3D electronic-innervated cells/tissues. Many 43  
 13 studies suggested that the organization, development, and 44  
 14 communication of cells are significantly different when 45  
 15 cultured/immobilized on 2-D substrates as compared with the 46  
 16 normal conditions in native 3-D matrix.<sup>109,110</sup> This difference 47  
 17 lead to bias/error in the *in-vitro* studies in cellular behaviors and 48  
 18 functions using planar bioelectronics. In tissue engineering, 350  
 19 cell cultures are popular approaches, which provide a biological 51  
 20 relevant microenvironment to ensure the normal behavior 52  
 21 of cells.<sup>111</sup> In order to enable the electrical access to these 353  
 22 cultured cellular networks, many hydrogel-based 354  
 23 electronics are developed. In 2019, Kalmykov et al. 55  
 24 demonstrated the use of self-rolling electrode arrays for 56  
 25 interfacing with 3-D hydrogel cardiac models (Fig. 7a,b).<sup>112</sup> The 57  
 26 3-D hydrogel creates a natural microenvironment by providing 58  
 27 a scaffold that allows biologically relevant cell-cell and cell- 59  
 28 matrix interaction, recapitulating the *in vivo* environment that 60  
 29 cannot be achieved in 2-D cell culture.<sup>113,114</sup> This allows for the 61  
 30 detection of biologically relevant behavior from *in vitro* models.<sup>62</sup>  
 31 Self-rolling the electrode array around the hydrogel spheroid 63  
 32 enables electrophysiological recording of 3-D signals.<sup>64</sup>

propagation (Fig. 7c). Similarly, Soscia et al. reported the use of 33  
 flexible 3-D microelectrode arrays for interfacing with and 34  
 recording from 3-D neuron cultures in collagen-based hydrogel 35  
 (Fig. 7d,e). The hydrogel cell culture creates an environment 36  
 that aims to recapitulate real brain function by facilitating cell- 37  
 cell communication and interactions. The flexible electrodes 38  
 could bend vertically 90 degrees in order to record in 3-D 39  
 hydrogels. After vertical alignment of electrodes, the 40  
 microelectrode arrays were seeded with human iPSC-derived 41  
 neurons and astrocytes in a collagen hydrogel containing 42  
 extracellular matrix proteins. Electrophysiological recordings 43  
 were conducted (Fig. 7f) and neurons were found to be viable 44  
 for over 30 days, demonstrating the potential for long-term 45  
 studies *in vitro*.<sup>101,102</sup>

Hydrogel electronics have also been exploited to improve 33  
 the electrical-to-biological signal transduction. Zhao et al. 34  
 developed an electronic circuit made of salt/PEG two-phase 35  
 hydrogels that is capable of effective modulation of cultured 36  
 neuron cells (SH-SY5Y) and skeletal muscle tissue.<sup>48</sup> In this 37  
 design, high ionic conductivity salt-solutions were stably 38  
 encapsulated within PEG hydrogel matrices. Patterning of the 39  
 hydrogel circuit enables control over ionic current for high 40  
 resolution stimulation both *in vitro* and *in vivo*. For *in vitro* 41  
 neuron cell stimulation, a hydrogel based electronic circuit 42  
 composed of four pairs of electrodes was applied, which 43  
 delivered  $3.6 \text{ V cm}^{-1}$  electrical field to cells for stimulation (Fig. 44  
 8 a and b). The results showed that the cells at the stimulated 45  
 spots exhibited higher intracellular calcium increase compared 46  
 to cells located at the resting spots, indicating successful cross- 47  
 system signal transduction. (Fig. 8c) For *in vivo* stimulation, a 48  
 hydrogel ionic stimulator made of one pair of electrodes was 49  
 interfaced with the tibialis anterior muscle at the knees of 50

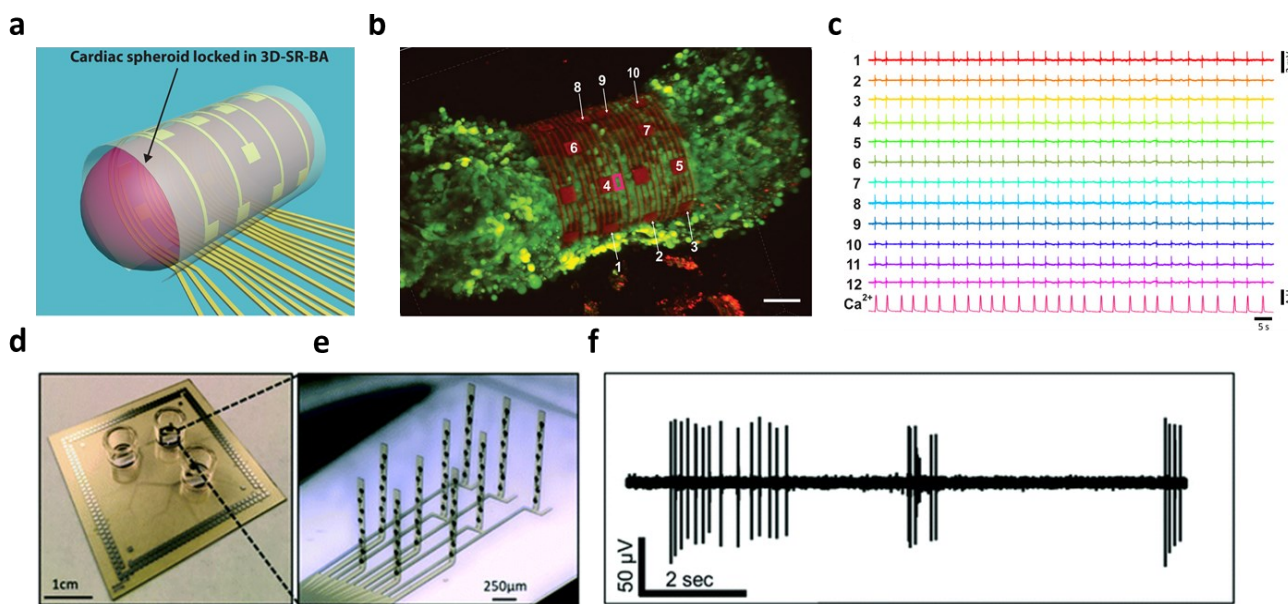


**Figure 7.** 3D electrode interface with 3D *in vitro* models. (a) 3D schematic of organoid interfacing with self-rolled biosensor array. (b) Confocal image of cardiac spheroid labeled with fluorescent calcium indicator. Scalebar, 50  $\mu\text{m}$ . (c) Field potential measurements from recording elements around the spheroid. Reproduced with permission from ref. 112. Copyright (2020) American Association for the Advancement of Science. (d,e) Image of device and closeup of bent electrodes. (f) Recording of neuronal activity in 3D culture from a single electrode. Reproduced with permission from ref. 101. Copyright (2020) The Royal Society of Chemistry.

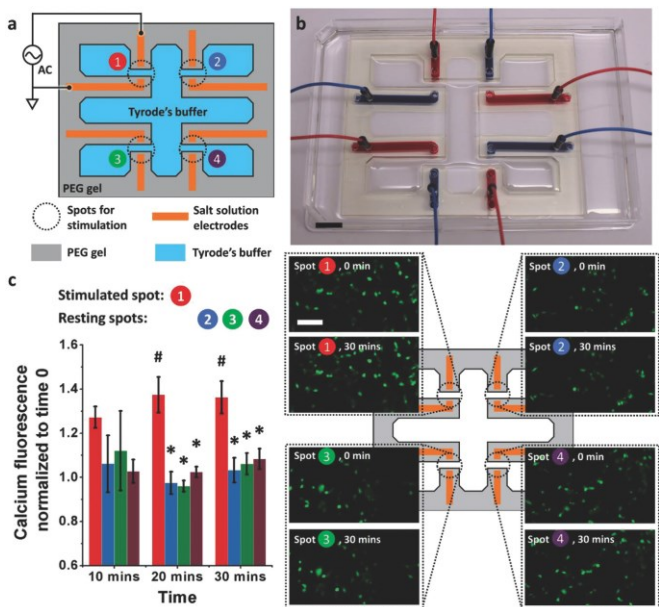


**Figure 8.** Hydrogel enabled bioelectronic interface for the manipulation of cellular functions (a) The schematic of the hydrogel ionic electrode array for *in vitro* neuron cell stimulation. (b) Image of the actual electronic circuit made of PEG hydrogel with 20% w/w PEGDMA 8000, 20% w/w PEGDA 700, and 1% w/w irgacure 2959. Scale bar, 1 cm. (c) Left: The intracellular calcium fluorescence change during stimulation (error bars indicate standard deviation,  $N = 3$ ). Spot 1 was stimulated, while the other spots were at rest. At 20 and 30 min, the fluorescence at stimulated spot (#) was significantly different than that at resting spots (\*) ( $p < 0.05$ ). Right: the corresponding fluorescence images at time 0 and 30 min at each spot. A higher fluorescence increase was seen at the stimulated spots. Scale bar = 100  $\mu$ m. Reproduced with permission from ref. 48. Copyright (2018) John Wiley & Sons, Inc.

two modular components: a microfluidic platform for media perfusion and glass plug-in with electrode components (Fig. 9a). The electrodes were functionalized with the enzymes: glucose oxidase or lactate oxidase immobilized in hydrogel, enabling the real time detection of cell metabolism. The device measured the real time secretion/consumption of analytes from the perfused cell media (Fig. 9b). Lian *et al.* reported the amperometric detection of hydrogen peroxide secreted from HeLa cells utilizing horseradish peroxidase (HRP) functionalized hydrogel coating on glassy carbon electrode (Fig. 9c).<sup>106</sup> HeLa cells were cultured on top of bioactive hydrogels, showing activity for up to two weeks. Cells were stimulated with Phorbol 12-myristate 13-acetate (PMA) to trigger hydrogen peroxide production. Horseradish peroxidase (HRP) was immobilized in the hydrogel, enabling the real time detection of hydrogen peroxide (Fig. 9d). The hydrogel also served to inhibit the diffusion of hydrogen peroxide secreted from cells, effectively increasing the concentration that directly interacts with HRP enzyme. Similar design has been applied by Yan *et al.* to study the metabolism of macrophage.<sup>105</sup> These works demonstrate the possibility for real time interpretation of cellular metabolic signals, which could be further expanded through incorporating different biomarkers and/or bioreceptors for real time drug screening, disease monitoring and personalized medicine.

#### 4.2 Wearable bioelectronics

Wearable bioelectronics are capable of real-time, noninvasive monitoring of physiological signals, and have become increasingly common in our everyday lives, e.g. in the form of smart watches/bands that can continuously measure heart rate or blood oxygen saturation.<sup>116</sup> However, these commercially available wearable devices share some similar challenges with metal/semiconductor based bioelectronics with unstable body contact that is associated with low sensitivity and fluctuation in sensing results.<sup>117</sup> To address this issue, flexible and stretchable electronics have been developed that comply with the curvatures of the human body; maintaining stable contacts to ensure consistent sensing results. Toward this goal, hydrogels are suggested as an ideal body-electronics interfacing material due to its superior mechanical property and tunable bio-adhesiveness. For example, Pan *et al.* reported hydrogel-elastomer composites with low stiffness and high adhesiveness for interfacing with skin.<sup>118</sup> Gold nanofilms were incorporated into the hydrogel structure for electrical conductivity and were demonstrated for on-skin electromyography and electrocardiography. The reported Young's modulus of the hydrogel composite was reported near 5.3 KPa and could stretch 25 times its length, enabling conformal contact with the skin. This work provides a general strategy for on-skin bioelectronics by engineering the hydrogel properties.

In wearable electronics, body motions are one of the most common challenges that can lead to device detachment, abrasion, fracture, and eventually failure of device functions. Recent studies in stretchable-, tough- and healable- hydrogels provide potential solutions to this challenge.<sup>119,120</sup> With further enhanced ionic conductivity, these novel hydrogels show

1 Sprague-Dawley rats. The stimulation results showed the force  
 2 generated from stimulation increased slightly from 300 mN at a  
 3 voltage of 0.9 V to a plateau of 380 mN with voltages of either  
 4 1.6 or 2.5 V. Additionally, compared with gold electrode,  
 5 lower voltage (2.5V vs. 4V) was required to generate a similar  
 6 force (1.38N vs 1.33N) when a hydrogel stimulator was used,  
 7 indicating more efficient electrical signal transmission/delivery.

8 Similarly, Liu *et al.* utilized micropatterned electrically  
 9 conductive hydrogels (MECH) to fabricate microelectrodes for  
 10 interfacing the nervous system of mice.<sup>22</sup> Owing to its electrical  
 11 and ionic conductivity as well as soft mechanical properties, the  
 12 MECH-based microelectrodes feature a contact impedance  
 13 >90% lower as compared with conductive hydrogel coated  
 14 electrode and >95% lower than silane-crosslinked PEDOT:PSS  
 15 coating. This low contact impedance enables the delivery of an  
 16 excitation current density as high as 10 mA·cm<sup>-2</sup> at a low voltage  
 17 of 50 mV, whereas the Pt electrode requires at least 500 mV to  
 18 achieve observable leg movements. The experimental results  
 19 demonstrated that MECH can locally stimulate the subgroups  
 20 peripheral nerve bundles to synchronize individual toe  
 21 movements with the stimulation frequency.

22 In terms of non-electroactive cells, most of their functions  
 23 are regulated by biochemical signals. The specific  
 24 electrical/electrochemical transduction of these signals relies  
 25 on the proper functioning and effective integration of bio  
 26 recognition molecules, where hydrogel could enable unique  
 27 possibilities to promote interfacial signaling as discussed earlier.  
 28 For instance, Misun *et al.* demonstrated the amperometric  
 29 detection of glucose consumption and lactate production from  
 30 human colon carcinoma spheroids.<sup>115</sup> The device consisted

1 potential to replace state-of-the-art substrates (e.g. metal<sup>26</sup>  
 2 semiconductor, dry polymer etc.) in the development of next<sup>27</sup>  
 3 generation wearable electronics. For example, Zhao et al.<sup>28</sup>  
 4 fabricated a conductive hydrogel from a supramolecular<sup>29</sup>  
 5 assembly of polydopamine decorated silver nanoparticles<sup>30</sup>  
 6 polyaniline, and polyvinyl alcohol. The conductive hydrogel<sup>31</sup>  
 7 displayed tunable stiffness (132 Pa to 40 kPa), stretchiness<sup>32</sup>  
 8 (0.01- 500%), self-adhesiveness and self-healing capacity, which<sup>33</sup>  
 9 is successfully implemented as epidermal motion sensors<sup>34</sup>  
 10 and diabetic wound dressing.<sup>121</sup> Also, Liu et al. created<sup>35</sup>  
 11 microfluidic-based, ultra-stretchable hydrogel network with<sup>36</sup>  
 12 metallic conductivity using liquid metal as conductive fillers.<sup>37</sup>  
 13 This device showed good stretchability and flexibility, which<sup>38</sup>  
 14 remain functional under many types of deformations (e.g. up to<sup>39</sup>  
 15 550% stretch, cyclic stretches, bends, and twists). Due to the<sup>40</sup>  
 16 metallic conductivity, this hydrogel can be applied in the<sup>41</sup>  
 17 fabrication of wireless bioelectronics for monitoring<sup>42</sup>  
 18 physiological conditions of human body using near-field<sup>43</sup>  
 19 communication technology. Furthermore, a variety of<sup>44</sup>  
 20 functional hydrogel designs for wearable electronics have been<sup>45</sup>  
 21 comprehensively reviewed by Yang and Suo.<sup>123</sup>

22 Additionally, multifunctional wearable hydrogel<sup>46</sup>  
 23 bioelectronics have been developed for simultaneous<sup>47</sup>  
 24 monitoring of the physiological environment and delivery<sup>48</sup>  
 25 drugs for treatment. For example, contact lenses are hydrogel-

based medical devices that have long been used to correct vision. By embedding sensors within the lens, smart contact lenses have been demonstrated for monitoring of diseases such as glaucoma and diabetes.<sup>124,125</sup> Keum et al. demonstrated contact lenses capable of monitoring glucose levels from tears in rabbits and delivery of the drugs metformin and genistein for treatment of hyperglycemia and diabetic retinopathy.<sup>126</sup> Similarly, a smart bandage was developed for monitoring of the wound environment and delivery of antibiotics.<sup>127</sup> Overall, hydrogel can create many new possibilities in wearable electronics owing to its programmable mechanical-, electrical-, and chemical- properties.<sup>128,129</sup>

## 5. Conclusions

Engineered hydrogel interfaces have shown great promise towards the seamless structural and functional integration between biological and electronic systems, which is transforming the design and development of next-generation bioelectronics across molecular, cellular, tissue and body levels. The mismatch at the heterogenous interface, both structurally and functionally, can be blurred by rationally programming the physiochemical parameters through controlled hydrogel synthesis/fabrication. In terms of structures, hydrogel provides

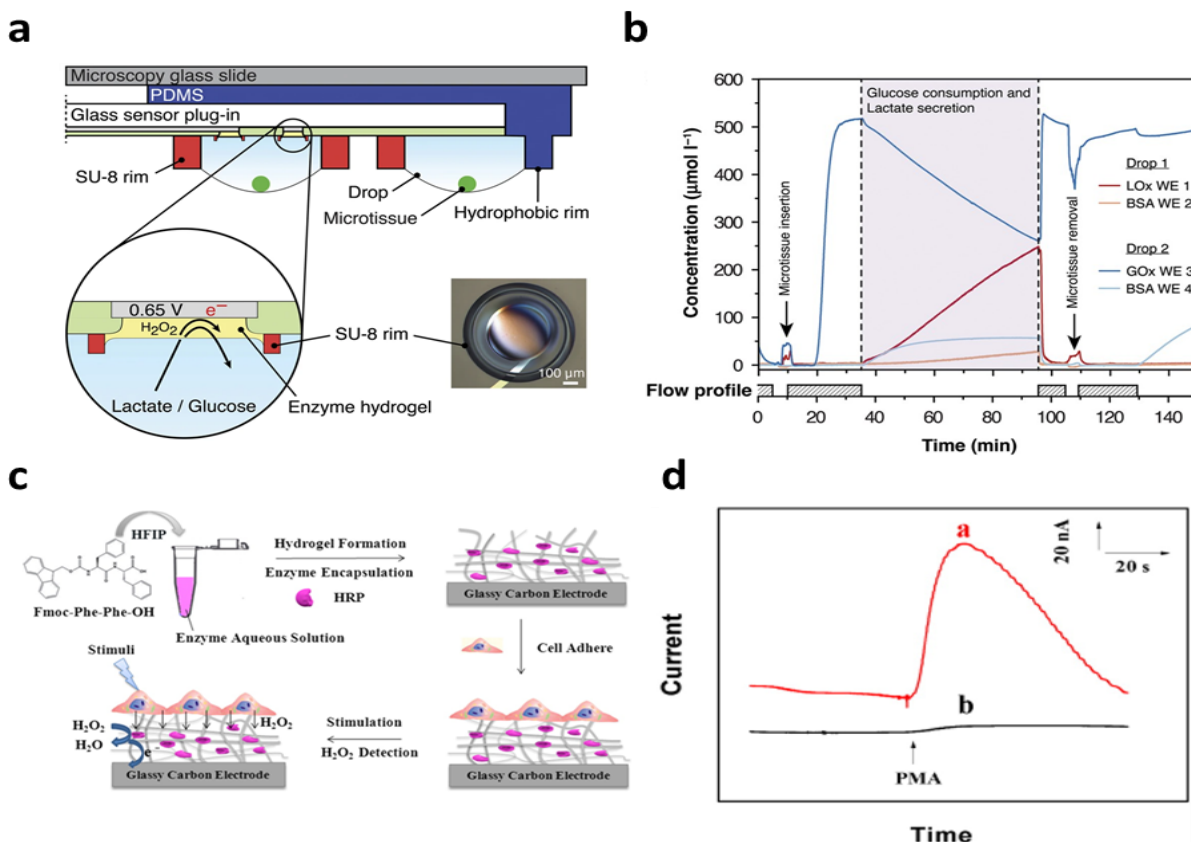


**Figure 9.** Hydrogel functionalization enables real time monitoring of cell metabolism. (a) Schematic of biosensor device with hanging drop networks for cell culture and hydrogels functionalized with lactate oxidase and glucose oxidase. (b) Real time monitoring of glucose consumption and lactate production. Reproduced with permission from ref. 115. Copyright (2016) Springer Nature. (c) Schematic of hydrogel formation and cell integration for electrochemical biosensing of  $\text{H}_2\text{O}_2$  after chemical stimuli. (d) Current response of sensor with (red) and without (black) HeLa cells after chemical stimulation. Reproduced with permission from ref. 106. Copyright (2016) American Chemical Society.

1 a mechanically compliant, chemically active, and biologically 1  
 2 favourable microenvironment for seamless bio-integration 52  
 3 that's difficult to achieve on traditional electronic interface. In 53  
 4 terms of functions, hydrogel can facilitate the signal 54  
 5 transduction between bio- (ions & molecules) and electrical 56  
 6 (electrons & holes) circuit by precisely regulating interface 57  
 7 mass and transport, enabling localized amplification and/or 58  
 8 filtering of bio-derived signals. At the molecular to cellular level, 59  
 9 the spatial organization and hierarchical assembling 60  
 10 functionalized hydrogels will create new signal transduction and 62  
 11 energy conversion cascades with electrically controllable inputs 63  
 12 and outputs for novel biosensor and biocatalysis 64  
 13 developments.<sup>130</sup> At the tissue to body level, recent 65  
 14 developments in stretchable-,<sup>131</sup> biodegradable-,<sup>132</sup> self- 66  
 15 healing-,<sup>133</sup> and bio-adhesive-hydrogels<sup>134</sup> offer opportunities 67  
 16 designing new bioelectronic interfaces with intimate contact, 68  
 17 minimal invasiveness, and maximized motion-compliance.<sup>69</sup> 70  
 18 Through these new bioelectronic interfaces, long term 72  
 19 continuous probing and regulation of human functions will be 73  
 20 achieved, which are expected to contribute significantly to 74  
 21 disease diagnosis and personalized medicine. Overall, we 75  
 22 believe that hydrogel-mediated bio-integratable electronics can 76  
 23 initiate an evolution in the way we communicate with biological 77  
 24 systems by unambiguously decoding critical biological 78  
 25 languages and precisely defining/regulating complex biological 79  
 26 functions.<sup>80</sup>

27 The future of hydrogel-based bioelectronics is anticipated to 82  
 28 implement more advanced functions beyond the current 83  
 29 scope of bioelectronics. However, before hydrogels can fully 84  
 30 address the interfacing challenges, more validation and 85  
 31 optimizations are required. Mainly, their long-term 86  
 32 performance and biocompatibility demand further evaluation 87  
 33 and optimization in order to obtain intimately integrated, yet 88  
 34 chronically stable bio-interfaces, which is critically important in 89  
 35 in-vivo and implanted applications. Other concerns include 90  
 36 degradation and potential cytotoxicity of different synthetic 91  
 37 hydrogels, as well as additional complexity and variability in 92  
 38 transducing and interpreting bioderived signals. In the long 93  
 39 term, given the ability to tune the physical and chemical 94  
 40 properties, biological interactions, and more, we are optimistic 95  
 41 for hydrogels potentials to address many challenges in 96  
 42 bioelectronics.<sup>97</sup>

43 **Conflicts of interest**

44 There are no conflicts to declare.

45 **Acknowledgements**

46 The authors gratefully acknowledge support from National 47 Science Foundation (CBET-1803907 and DMR-1652095).

48 **References**

49 1 J. Wang, *Chem. Rev.*, 2008, **108**, 814–825.  
 50 2 H. Berger, *Archiv f. Psychiatrie*, 1929, **87**, 527–570.

51 3 M. AlGhatrif and J. Lindsay, *Journal of Community Hospital Internal Medicine Perspectives*, 2012, **2**, 14383.  
 52 4 O. Aquilina, *Images Paediatr Cardiol*, 2006, **8**, 17–81.  
 53 5 J. Gardner, *Soc Stud Sci*, 2013, **43**, 707–728.  
 54 6 J. P. Seymour, F. Wu, K. D. Wise and E. Yoon, *Microsystems & Nanoengineering*, 2017, **3**, 1–16.  
 55 7 T. Yeung, P. C. Georges, L. A. Flanagan, B. Marg, M. Ortiz, M. Funaki, N. Zahir, W. Ming, V. Weaver and P. A. Janmey, *Cell Motility*, 2005, **60**, 24–34.  
 56 8 M. HajjHassan, V. Chodavarapu and S. Musallam, *Sensors*, 2008, **8**, 6704–6726.  
 57 9 V. S. Polikov, P. A. Tresco and W. M. Reichert, *Journal of Neuroscience Methods*, 2005, **148**, 1–18.  
 58 10 N. Wisniewski, F. Moussy and W. M. Reichert, *Fresenius J Anal Chem*, 2000, **366**, 611–621.  
 59 11 R. C. Kelly, M. A. Smith, J. M. Samonds, A. Kohn, A. B. Bonds, J. A. Movshon and T. S. Lee, *J. Neurosci.*, 2007, **27**, 261–264.  
 60 12 A. Zhang and C. M. Lieber, *Chem. Rev.*, 2016, **116**, 215–257.  
 61 13 T. Zhou, G. Hong, T.-M. Fu, X. Yang, T. G. Schuhmann, R. D. Viveros and C. M. Lieber, *Proc Natl Acad Sci USA*, 2017, **114**, 5894–5899.  
 62 14 M. E. Spira and A. Hai, *Nature Nanotechnology*, 2013, **8**, 83–94.  
 63 15 N. Gao, W. Zhou, X. Jiang, G. Hong, T.-M. Fu and C. M. Lieber, *Nano Lett.*, 2015, **15**, 2143–2148.  
 64 16 A. S. Hoffman, *Advanced Drug Delivery Reviews*, 2012, **64**, 18–23.  
 65 17 H. Yuk, B. Lu and X. Zhao, *Chemical Society Reviews*, 2019, **48**, 1642–1667.  
 66 18 S. Lin, C. Cao, Q. Wang, M. Gonzalez, J. E. Dolbow and X. Zhao, *Soft Matter*, 2014, **10**, 7519–7527.  
 67 19 B. Xu, P. Zheng, F. Gao, W. Wang, H. Zhang, X. Zhang, X. Feng and W. Liu, *Advanced Functional Materials*, 2017, **27**, 1604327.  
 68 20 J. L. Drury and D. J. Mooney, *Biomaterials*, 2003, **24**, 4337–4351.  
 69 21 Y. Liu, W. He, Z. Zhang and B. P. Lee, *Gels*, 2018, **4**, 46.  
 70 22 Y. Liu, J. Liu, S. Chen, T. Lei, Y. Kim, S. Niu, H. Wang, X. Wang, A. M. Foudeh, J. B.-H. Tok and Z. Bao, *Nature Biomedical Engineering*, 2019, **3**, 58–68.  
 71 23 J. Yang, R. Bai, B. Chen and Z. Suo, *Advanced Functional Materials*, 2020, **30**, 1901693.  
 72 24 D. Gao, K. Parida and P. S. Lee, *Advanced Functional Materials*, 2020, **30**, 1907184.  
 73 25 Y. S. Zhang and A. Khademhosseini, *Science*, 2017, **356**, eaaf3627.  
 74 26 X. Li, Q. Sun, Q. Li, N. Kawazoe and G. Chen, *Frontiers in Chemistry*, 2018, **6**, 499.  
 75 27 J. Yan, V. A. Pedrosa, A. L. Simonian and A. Revzin, *ACS Appl Mater Interfaces*, 2010, **2**, 748–755.  
 76 28 J. Chen, Q. Peng, T. Thundat and H. Zeng, *Chem. Mater.*, 2019, **31**, 4553–4563.  
 77 29 N. A. Alba, R. J. Scibassi, M. Sun and X. T. Cui, *IEEE Transactions on Neural Systems and Rehabilitation Engineering*, 2010, **18**, 415–423.  
 78 30 S. Ji, C. Wan, T. Wang, Q. Li, G. Chen, J. Wang, Z. Liu, H. Yang, X. Liu and X. Chen, *Advanced Materials*, 2020, **32**, 2001496.  
 79 31 M. Baumgartner, F. Hartmann, M. Drack, D. Preninger, D. Wirthl, R. Gerstmayr, L. Lehner, G. Mao, R. Pruckner, S. Demchyshyn, L. Reiter, M. Strobel, T. Stockinger, D. Schiller, S. Kimeswenger, F. Greibich, G. Buchberger, E. Bradt, S. Hild, S. Bauer and M. Kaltenbrunner, *Nature Materials*, 2020, 1–8.  
 80 32 Z. Taylor and K. Miller, *Journal of Biomechanics*, 2004, **37**, 1263–1269.  
 81 33 W. Hiesinger, M. J. Brukman, R. C. McCormick, J. R. Fitzpatrick, J. R. Frederick, E. C. Yang, J. R. Muenzer, N. A. Marotta, M. F. Berry, P. Atluri and Y. J. Woo, *J. Thorac. Cardiovasc. Surg.*, 2012, **143**, 962–966.

1 34 B. Wang, W. Huang, L. Chi, M. Al-Hashimi, T. J. Marks and **68** 62 N. R. Mohamad, N. H. C. Marzuki, N. A. Buang, F. Huyop and  
2 Facchetti, *Chem. Rev.*, 2018, **118**, 5690–5754. **69** 69 R. A. Wahab, *Biotechnol Biotechnol Equip*, 2015, **29**, 205–220.  
3 35 S. R. Goldstein and M. Salzman, *IEEE Transactions **70** 63 U. Guzik, K. Hupert-Kocurek and D. Wojcieszyska, *Molecules*,  
4 Biomedical Engineering*, 1973, **BME-20**, 260–269. **71** 2014, **19**, 8995–9018.  
5 36 J. W. Salatino, K. A. Ludwig, T. D. Y. Kozai and E. K. Purcell **72** 64 E. Stern, R. Wagner, F. J. Sigworth, R. Breaker, T. M. Fahmy  
6 *Nature Biomedical Engineering*, 2017, **1**, 862–877. **73** 73 and M. A. Reed, *Nano Lett.*, 2007, **7**, 3405–3409.  
7 37 A. Prasad and J. C. Sanchez, *J. Neural Eng.*, 2012, **9**, 026028. **74** 65 G. Zheng, F. Patolsky, Y. Cui, W. U. Wang and C. M. Lieber,  
8 38 K. Woepel, Q. Yang and X. T. Cui, *Curr Opin Biomed Eng* **75** 2005, **23**, 1294–1301.  
9 2017, **4**, 21–31. **76** 66 R. Elnathan, M. Kwiat, A. Pevzner, Y. Engel, L. Burstein, A.  
10 39 J. Goding, A. Gilmour, P. Martens, L. Poole-Warren and **77** A. Khatchourint, A. Lichtenstein, R. Kantaev and F. Patolsky,  
11 Green, *Advanced Healthcare Materials*, 2017, **6**, 1601177. **78** **72** *Nano Lett.*, 2012, **12**, 5245–5254.  
12 40 L. Ferlauto, A. N. D'Angelo, P. Vagni, M. J. I. Airaghi Leccardi **79** 67 N. Nakatsuka, K.-A. Yang, J. M. Abendroth, K. M. Cheung, X.  
13 F. M. Mor, E. A. Cutta, M. O. Heuschkel, L. Stoppini and **80** 81 Xu, H. Yang, C. Zhao, B. Zhu, Y. S. Rim, Y. Yang, P. S. Weiss, M.  
14 Ghezzi, *Frontiers in Neuroscience*, 2018, **12**, 648. **81** N. Stojanović and A. M. Andrews, *Science*, 2018, **362**, 319–  
15 41 R. G. Wells, *Hepatology*, 2008, **47**, 1394–1400. **82** 324.  
16 42 A. J. Engler, C. Carag-Krieger, C. P. Johnson, M. Raab, H. **83** 68 N. Kumar, M. Gray, J. C. Ortiz-Marquez, A. Weber, C. R.  
17 Tang, D. W. Speicher, J. W. Sanger, J. M. Sanger and D. **84** 69 Desmond, A. Argun, T. van Opijken and K. S. Burch, *bioRxiv*,  
18 Discher, *Journal of Cell Science*, 2008, **121**, 3794–3802. **85** 2020, preprint, <https://doi.org/10.1101/2020.05.22.111047>.  
19 43 K. C. Spencer, J. C. Sy, K. B. Ramadi, A. M. Graybiel, R. Lang **86** 69 J. E. Contreras-Naranjo and O. Aguilar, *Biosensors (Basel)*,  
20 and M. J. Cima, *Scientific Reports*, 2017, **7**, 1–16. **87** 2019, **9**, 15.  
21 44 J. D. Enderle, in *Introduction to Biomedical Engineering (Third **88** 70 P. Roach, D. Farrar and C. C. Perry, *J. Am. Chem. Soc.*, 2005,  
22 Edition)*, eds. J. D. Enderle and J. D. Bronzino, Academic Pre **89** **127**, 8168–8173.  
23 Boston, 2012, Chapter 8, pp. 447–508. **90** 71 Y. Li, T. L. Ogorzalek, S. Wei, X. Zhang, P. Yang, J. Jasensky, C.  
24 45 M. Escabé, in *Introduction to Biomedical Engineering (Third **91** 72 L. Brooks, E. N. G. Marsh and Z. Chen, *Phys. Chem. Chem.  
25 Edition)*, eds. J. D. Enderle and J. D. Bronzino, Academic Pre **92** Phys.*, 2018, **20**, 1021–1029.  
26 Boston, 2012, Chapter 11, pp. 667–746. **93** 72 S. Datta, L. R. Christena and Y. R. S. Rajaram, *3 Biotech*, 2013,  
27 46 J. D. Enderle, in *Introduction to Biomedical Engineering (Third **94** **3**, 1–9.  
28 Edition)*, eds. J. D. Enderle and J. D. Bronzino, Academic Pre **95** 73 J. Tavakoli and Y. Tang, *Polymers*, 2017, **9**, 364.  
29 Boston, 2012, Chapter 12, pp. 747–815. **96** 74 N. Gao, T. Gao, X. Yang, X. Dai, W. Zhou, A. Zhang and C. M.  
30 47 C.-J. Lee, H. Wu, Y. Hu, M. Young, H. Wang, D. Lynch, F. Xu, **97** 75 Lieber, *Proc Natl Acad Sci USA*, 2016, **113**, 14633–14638.  
31 Cong and G. Cheng, *ACS Appl. Mater. Interfaces*, 2018, **10**, **98** 75 X. Dai, R. Vo, H.-H. Hsu, P. Deng, Y. Zhang and X. Jiang, *Nano  
32 5845–5852. **99** Lett.*, 2019, **19**, 6658–6664.  
33 48 S. Zhao, P. Tseng, J. Grasman, Y. Wang, W. Li, B. Napier **100** 76 H. H. Bay, R. Vo, X. Dai, H.-H. Hsu, Z. Mo, S. Cao, W. Li, F. G.  
34 Yavuz, Y. Chen, L. Howell, J. Rincon, F. G. Omenetto and **101** 76 Omenetto and X. Jiang, *Nano Lett.*, 2019, **19**, 2620–2626.  
35 Kaplan, *Advanced Materials*, 2018, **30**, 1800598. **102** 77 J. Kunkel and P. Asuri, *PLOS ONE*, 2014, **9**, e86785.  
36 49 I. Noshadi, B. W. Walker, R. Portillo-Lara, E. Shirzaei Sani **103** 78 D. P. Hickey, R. C. Reid, R. D. Milton and S. D. Minteer,  
37 Gomes, M. R. Azizian and N. Annabi, *Scientific Reports*, 2014, **104** 78 *Biosensors and Bioelectronics*, 2016, **77**, 26–31.  
38 **7**, 4345. **105** 79 J. Kim, I. Jeerapan, S. Imani, T. N. Cho, A. Bandodkar, S. Cinti,  
39 50 H. Jo, M. Sim, S. Kim, S. Yang, Y. Yoo, J.-H. Park, T. H. Yoon, **106** 80 P. P. Mercier and J. Wang, *ACS Sens.*, 2016, **1**, 1011–1019.  
40 G. Kim and J. Y. Lee, *Acta Biomaterialia*, 2017, **48**, 100–104. **107** 80 A. J. Bandodkar, W. Jia, C. Yardimci, X. Wang, J. Ramirez and J.  
41 51 X. Liu, A. L. Miller, S. Park, B. E. Waletzki, Z. Zhou, A. Terzic **108** 81 Wang, *Anal. Chem.*, 2015, **87**, 394–398.  
42 L. Lu, *ACS Appl. Mater. Interfaces*, 2017, **9**, 14677–14690. **109** 81 L. Li, L. Pan, Z. Ma, K. Yan, W. Cheng, Y. Shi and G. Yu, *Nano  
43 52 P. Baei, S. Jalili-Firoozinezhad, S. Rajabi-Zeleti, M. Tafazz **110** Lett.*, 2018, **18**, 3322–3327.  
44 Shadpour, H. Baharvand and N. Aghdam, *Materials **111** 82 M. J. Schöning and A. Poghossian, *Analyst*, 2002, **127**, 1137–  
45 and Engineering: C*, 2016, **63**, 131–141. **112** 1151.  
46 53 L. Xu, X. Li, T. Takemura, N. Hanagata, G. Wu and L. L. Cho **113** 83 Y. Maeda, A. Matsumoto, Y. Miura and Y. Miyahara,  
47 *Nanobiotechnology*, 2012, **10**, 16. **114** 2012, **7**, 108.  
48 54 A. N. Dalrymple, U. A. Robles, M. Huynh, B. A. Nayagam, R. **115** 84 T. Miyata, N. Asami and T. Uragami, *Nature*, 1999, **399**, 766–  
49 Green, L. A. Poole-Warren, J. B. Fallon and R. K. Shepherd **116** 769.  
50 *Neural Eng.*, 2020, **17**, 026018. **117** 85 T. Aoki, K. Nakamura, K. Sanui, A. Kikuchi, T. Okano, Y. Sakurai  
51 55 Y. Liu, A. F. McGuire, H.-Y. Lou, T. L. Li, J. B.-H. Tok, B. Cui **118** 86 and N. Ogata, *Polymer Journal*, 1999, **31**, 1185–1188.  
52 Z. Bao, *Proc Natl Acad Sci USA*, 2018, **115**, 11718–11723. **119** 86 K. Podual, F. J. Doyle and N. A. Peppas, *Journal of Controlled  
53 56 V. R. Feig, H. Tran, M. Lee and Z. Bao, *Nature Communications* **120** **121** 87 Release, 2000, **67**, 9–17.  
54 2018, **9**, 2740. **121** 87 P. B. Welzel, S. Prokoph, A. Zieris, M. Grimmer, S. Zschoche,  
55 57 H. Yuk, B. Lu, S. Lin, K. Qu, J. Xu, J. Luo and X. Zhao, *Nature **122** 88 U. Freudenberg and C. Werner, *Polymers*, 2011, **3**, 602–620.  
56 Communications*, 2020, **11**, 1–8. **123** 88 H. Chavda and C. Patel, *Int J Pharm Investig*, 2011, **1**, 17–21.  
57 58 J. Liu, X. Zhang, Y. Liu, M. Rodrigo, P. D. Loftus, J. Aparicio **124** 89 N. W. Choi, J. Kim, S. C. Chapin, T. Duong, E. Donohue, P.  
58 Valenzuela, J. Zheng, T. Pong, K. J. Cyr, M. Babakhanian **125** 89 Pandey, W. Broom, W. A. Hill and P. S. Doyle, *Anal. Chem.*,  
59 Hasi, J. Li, Y. Jiang, C. J. Kenney, P. J. Wang, A. M. Lee and **126** 2012, **84**, 9370–9378.  
60 Bao, *Proc Natl Acad Sci USA*, 2020, **117**, 14769. **127** 90 S. L. Burrs, D. C. Vanegas, M. Bhargava, N. Mechulani, P.  
61 59 D. N. Heo, S.-J. Song, H.-J. Kim, Y. J. Lee, W.-K. Ko, S. J. Lee **128** 90 Hendershot, H. Yamaguchi, C. Gomes and E. S. McLamore,  
62 Lee, S. J. Park, L. G. Zhang, J. Y. Kang, S. H. Do, S. H. Lee and **129** 2015, **140**, 1466–1476.  
63 K. Kwon, *Acta Biomaterialia*, 2016, **39**, 25–33. **130** 91 H. J. Kim, W. Choi, J. Kim, J. Choi, N. Choi and K. S. Hwang,  
64 60 N. J. Ronkainen, H. B. Halsall and W. R. Heineman, *Chem. **131** 91 *Sensors and Actuators B: Chemical*, 2020, **302**, 127190.  
65 Rev.*, 2010, **39**, 1747–1763. **132** 92 R. J. Russell, A. C. Axel, K. L. Shields and M. V. Pishko, *Polymer*,  
66 61 W. Schramm, S.-H. Paek and G. Voss, *ImmunoMethods*, 1993 **133** 2001, **42**, 4893–4901.  
67 3, 93–103. **134** 93 B. Amsden, *Macromolecules*, 1998, **31**, 8382–8395.*

1 94 E. Axpe, D. Chan, G. S. Offeddu, Y. Chang, D. Merida, H. **67** 120 T. Kakuta, Y. Takashima, M. Nakahata, M. Otsubo, H.  
 2 Hernandez and E. A. Appel, *Macromolecules*, 2019, **52**, 6886–6897. **68** 69 Yamaguchi and A. Harada, *Advanced Materials*, 2013, **25**,  
 3 6897. **70** 2849–2853.  
 4 95 A. Star, E. Tu, J. Niemann, J.-C. P. Gabriel, C. S. Joiner and **70** 121 Y. Zhao, Z. Li, S. Song, K. Yang, H. Liu, Z. Yang, J. Wang, B. Yang  
 5 Valcke, *Proc Natl Acad Sci USA*, 2006, **103**, 921–926. **71** and Q. Lin, *Advanced Functional Materials*, 2019, **29**,  
 6 96 E. Stern, J. F. Klemic, D. A. Routenberg, P. N. Wyrembak, D. **72** 1901474.  
 7 Turner-Evans, A. D. Hamilton, D. A. LaVan, T. M. Fahmy and **73** 122 Y. Liu, T. Yang, Y. Zhang, G. Qu, S. Wei, Z. Liu and T. Kong,  
 8 M. A. Reed, *Nature*, 2007, **445**, 519–522. **74** *Advanced Materials*, 2019, **31**, 1902783.  
 9 97 F. Patolsky, G. Zheng, O. Hayden, M. Lakadamyali, X. Zhuang **75** 123 C. Yang and Z. Suo, *Nature Reviews Materials*, 2018, **3**, 125–  
 10 and C. M. Lieber, *Proc Natl Acad Sci USA*, 2004, **101**, 14017–14022. **76** 142.  
 11 77 124 G. E. Dunbar, B. Y. Shen and A. A. Aref, *Clin Ophthalmol*, 2017, **11**, 875–882.  
 12 98 G. L. Mario Cheong, K. S. Lim, A. Jakubowicz, P. J. Martens, **78** 125 M. Senior, *Nature Biotechnology*, 2014, **32**, 856–856.  
 13 A. Poole-Warren and R. A. Green, *Acta Biomater*, 2014, **109** 126 D. H. Keum, S.-K. Kim, J. Koo, G.-H. Lee, C. Jeon, J. W. Mok, B.  
 14 1216–1226. **80** H. Mun, K. J. Lee, E. Kamrani, C.-K. Joo, S. Shin, J.-Y. Sim, D.  
 15 99 J. O. Winter, S. F. Cogan and J. F. Rizzo, *J. Biomed. Mater. Res. Part B Appl. Biomater.*, 2007, **81**, 551–563. **82** Myung, S. H. Yun, Z. Bao and S. K. Hahn, *Science Advances*,  
 16 100 M. L. McCain, A. Agarwal, H. W. Nesmith, A. P. Nesmith and **83** 2020, **6**, eaba3252.  
 17 K. Parker, *Biomaterials*, 2014, **35**, 5462–5471. **84** 127 P. Mostafalu, A. Tamayol, R. Rahimi, M. Ochoa, A. Khalilpour,  
 18 101 D. A. Soscia, D. Lam, A. C. Tooker, H. A. Enright, M. Triplett, **85** G. Kiaee, I. K. Yazdi, S. Bagherifard, M. R. Dokmeci, B. Ziaie, S.  
 19 Karande, S. K. G. Peters, A. P. Sales, E. K. Wheeler and N. **86** R. Sonkusale and A. Khademhosseini, *Small*, 2018, **14**,  
 20 Fischer, *Lab Chip*, 2020, **20**, 901–911. **87** 1703509.  
 21 102 D. Lam, H. A. Enright, S. K. G. Peters, M. L. Moya, D. A. Soscia, **88** 128 Z. Lou, L. Wang, K. Jiang, Z. Wei and G. Shen, *Materials Science  
 22 89 J. Cadena, J. A. Alvarado, K. S. Kulp, E. K. Wheeler and N. **89** and Engineering: R: Reports*, 2020, **140**, 100523.  
 23 Fischer, *Journal of Neuroscience Methods*, 2020, **329**, 1084600  
 24 103 S. Lee, D. Sasaki, D. Kim, M. Mori, T. Yokota, H. Lee, S. Park, **91** 129 J. C. Yang, J. Mun, S. Y. Kwon, S. Park, Z. Bao and S. Park,  
 25 Fukuda, M. Sekino, K. Matsuura, T. Shimizu and T. Someya, **92** *Advanced Materials*, 2019, **31**, 1904765.  
 26 *Nature Nanotechnology*, 2019, **14**, 156–160. **93** 130 L. Hsu and X. Jiang, *Trends in Biotechnology*, 2019, **37**, 795–  
 27 104 V. J. Kujala, F. S. Pasqualini, J. A. Goss, J. C. Nawroth and K. **94** 131 H. Liu, M. Li, C. Ouyang, T. J. Lu, F. Li and F. Xu, *Small*, 2018,  
 28 Parker, *J. Mater. Chem. B*, 2016, **4**, 3534–3543. **95** **14**, 1801711.  
 29 105 J. Yan, Y. Sun, H. Zhu, L. Marcu and A. Revzin, *Biosensors and **100** 132 B. Guo, A. Finne-Wistrand and A.-C. Albertsson, *Chem. Mater.*,  
 30 **96** *Bioelectronics*, 2009, **24**, 2604–2610. **97** 2011, **23**, 1254–1262.  
 31 106 M. Lian, X. Chen, Y. Lu and W. Yang, *ACS Appl. Mater. **101** 133 Z. Deng, H. Wang, P. X. Ma and B. Guo, *Nanoscale*, 2020, **12**,  
 32 **98** *Interfaces*, 2016, **8**, 25036–25042. **99** 1224–1246.  
 33 107 M. Kitsara, D. Kontziamasis, O. Agbulut and Y. Chai, **102** 134 H. Chopra, S. Kumar and I. Singh, in *Bioadhesives in Drug  
 34 *Microelectronic Engineering*, 2019, **203–204**, 44–62. **103** *Delivery*, John Wiley & Sons, Ltd, 2020, Chapter 6, pp. 147–  
 35 108 P. Fattah, G. Yang, G. Kim and M. R. Abidian, *Advanc. **104** 170.*  
 36 **102** *Materials*, 2014, **26**, 1846–1885. **103**  
 37 109 J. L. Bourke, A. F. Quigley, S. Duchi, C. D. O'Connell, J. M. **105**  
 38 Crook, G. G. Wallace, M. J. Cook and R. M. I. Kapsa, *Journal of **106***  
 39 *Tissue Engineering and Regenerative Medicine*, 2018, **104**  
 40 490–493.  
 41 110 S. P. Paşa, *Nature*, 2018, **553**, 437–445.  
 42 111 R. Edmondson, J. J. Broglie, A. F. Adcock and L. Yang, *ASSAY **107***  
 43 and *Drug Development Technologies*, 2014, **12**, 207–218.  
 44 112 A. Kalmynov, C. Huang, J. Bliley, D. Shiwartska, J. Tashman, A. **108**  
 45 Abdullah, S. K. Rastogi, S. Shukla, E. Mataev, A. W. Feinberg, **109**  
 46 K. J. Hsia and T. Cohen-Karni, *Science Advances*, 2019, **5**, **110**  
 47 eaax0729.  
 48 113 A. P. Napolitano, D. M. Dean, A. J. Man, J. Youssef, D. N. Ho, **111**  
 49 A. P. Rago, M. P. Lech and J. R. Morgan, *BioTechniques*, 2007, **112**  
 50 **43**, 494–500.  
 51 114 M. W. Tibbitt and K. S. Anseth, *Biotechnol Bioeng*, 2009, **103**, **113**  
 52 655–663.  
 53 115 P. M. Misun, J. Rothe, Y. R. F. Schmid, A. Hierlemann and O. **114**  
 54 Frey, *Microsystems & Nanoengineering*, 2016, **2**, 1–9.  
 55 116 D. Phan, L. Y. Siong, P. N. Pathirana and A. Seneviratne, in **115**  
 56 2015 *International Symposium on Bioelectronics and Bioinformatics **116***  
 57 (ISBB), 2015, pp. 144–147.  
 58 117 Z. Lou, L. Wang and G. Shen, *Advanced Materials **117***  
 59 **118** *Technologies*, 2018, **3**, 1800444.  
 60 118 S. Pan, F. Zhang, P. Cai, M. Wang, K. He, Y. Luo, Z. Li, G. Chen, **119**  
 61 S. Ji, Z. Liu, X. J. Loh and X. Chen, *Advanced Functional **120***  
 62 **119** *Materials*, **26**, 1909540.  
 63 119 J.-Y. Sun, X. Zhao, W. R. K. Illeperuma, O. Chaudhuri, K. H. Oh, **121**  
 64 D. J. Mooney, J. J. Vlassak and Z. Suo, *Nature*, 2012, **489**, 133–  
 65 136.  
 66 136.***